Shallow magma reservoirs as elastic-plated gravity currents

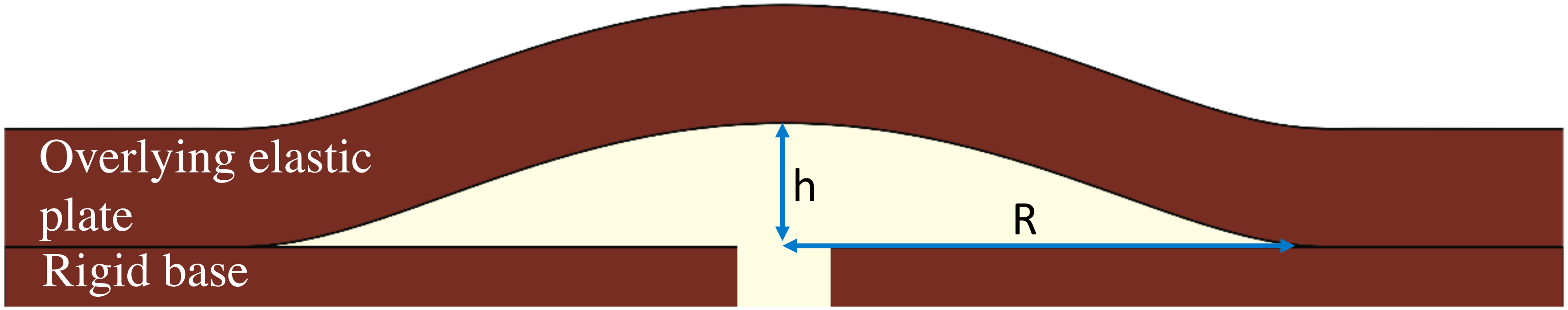

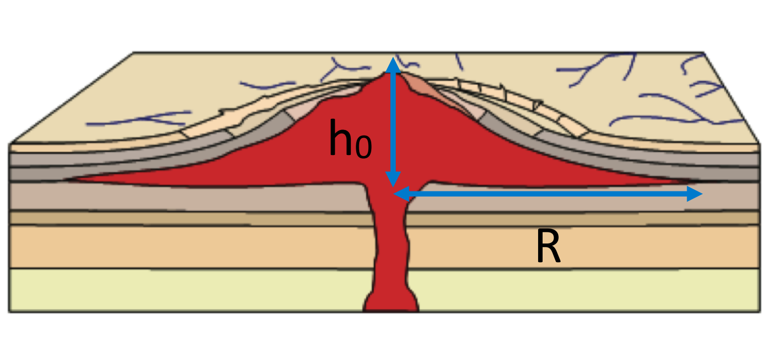

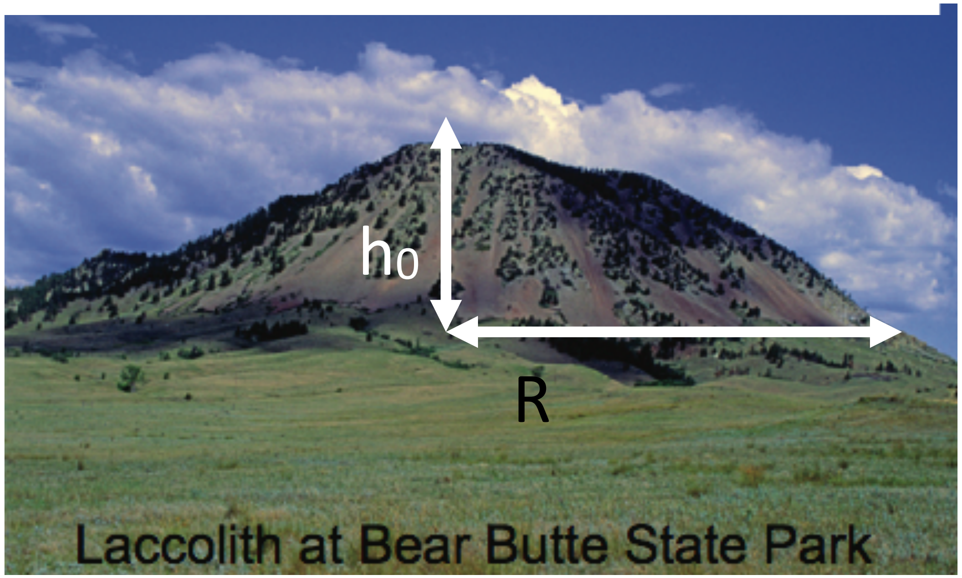

Chloé Michaut
ENS Lyon

Magmatic intrusions

1/ Laccolith
5/ Sill
4/ Dyke

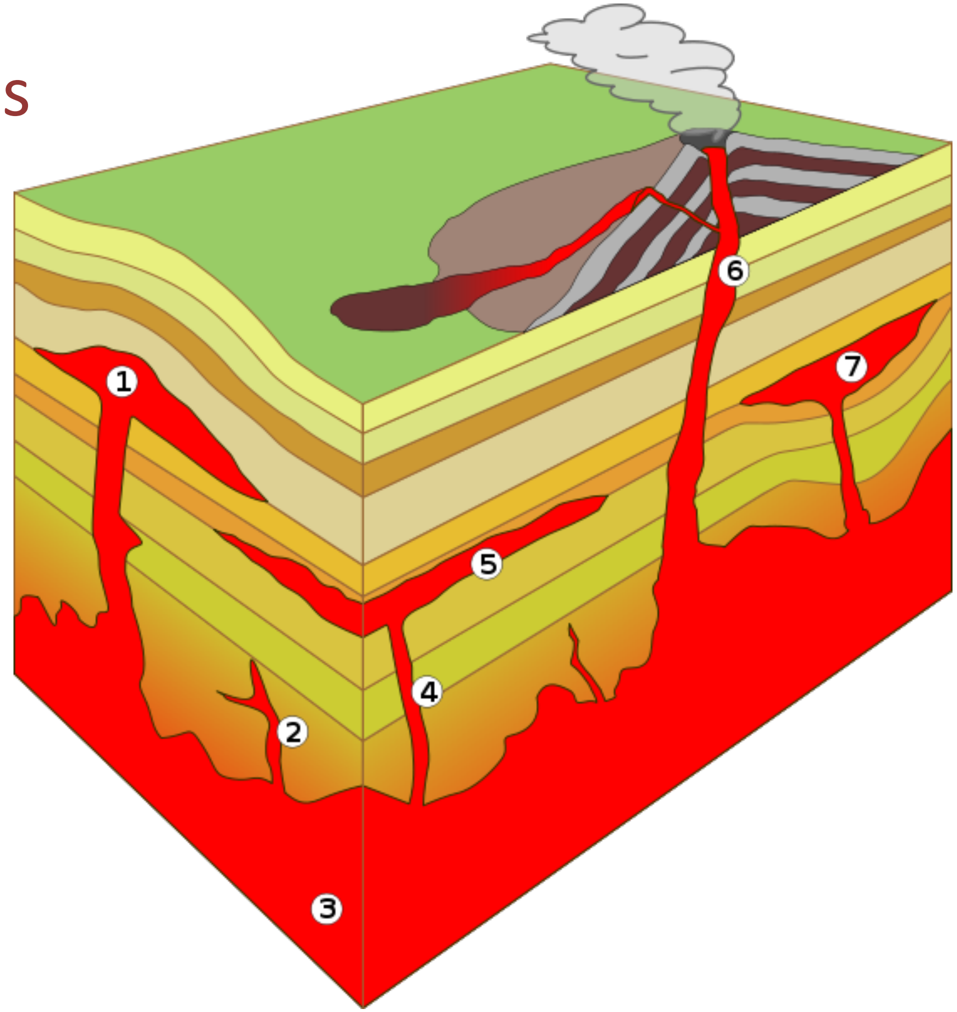

Magma ascent in the crust depends on:

- magma buoyancy
- the state of stress

in the crust.

Laccoliths : shallow intrusions spreading as elastic-plated gravity currents

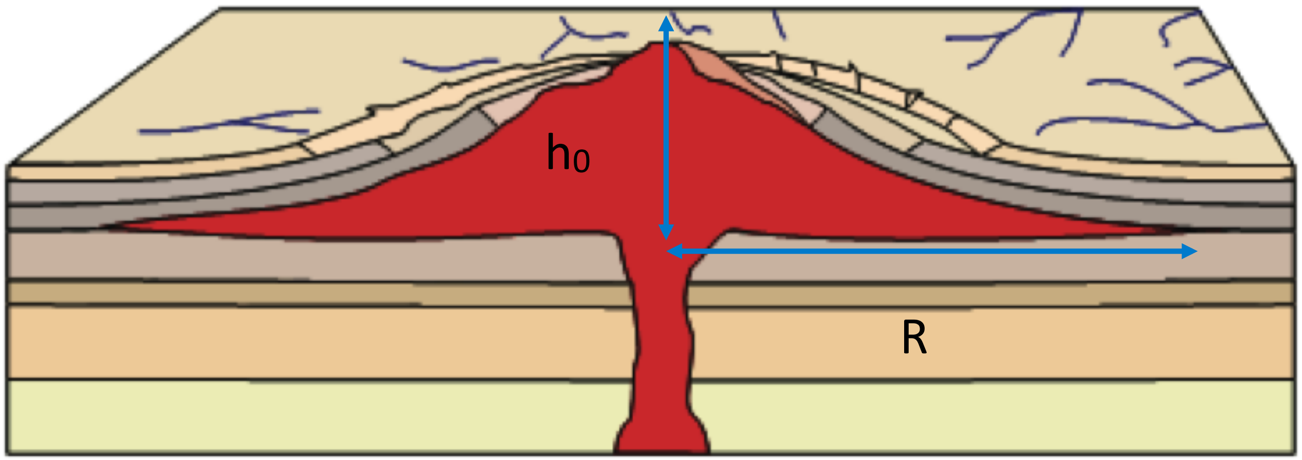

Flow of water below ice sheet: lake drainage in Greenland

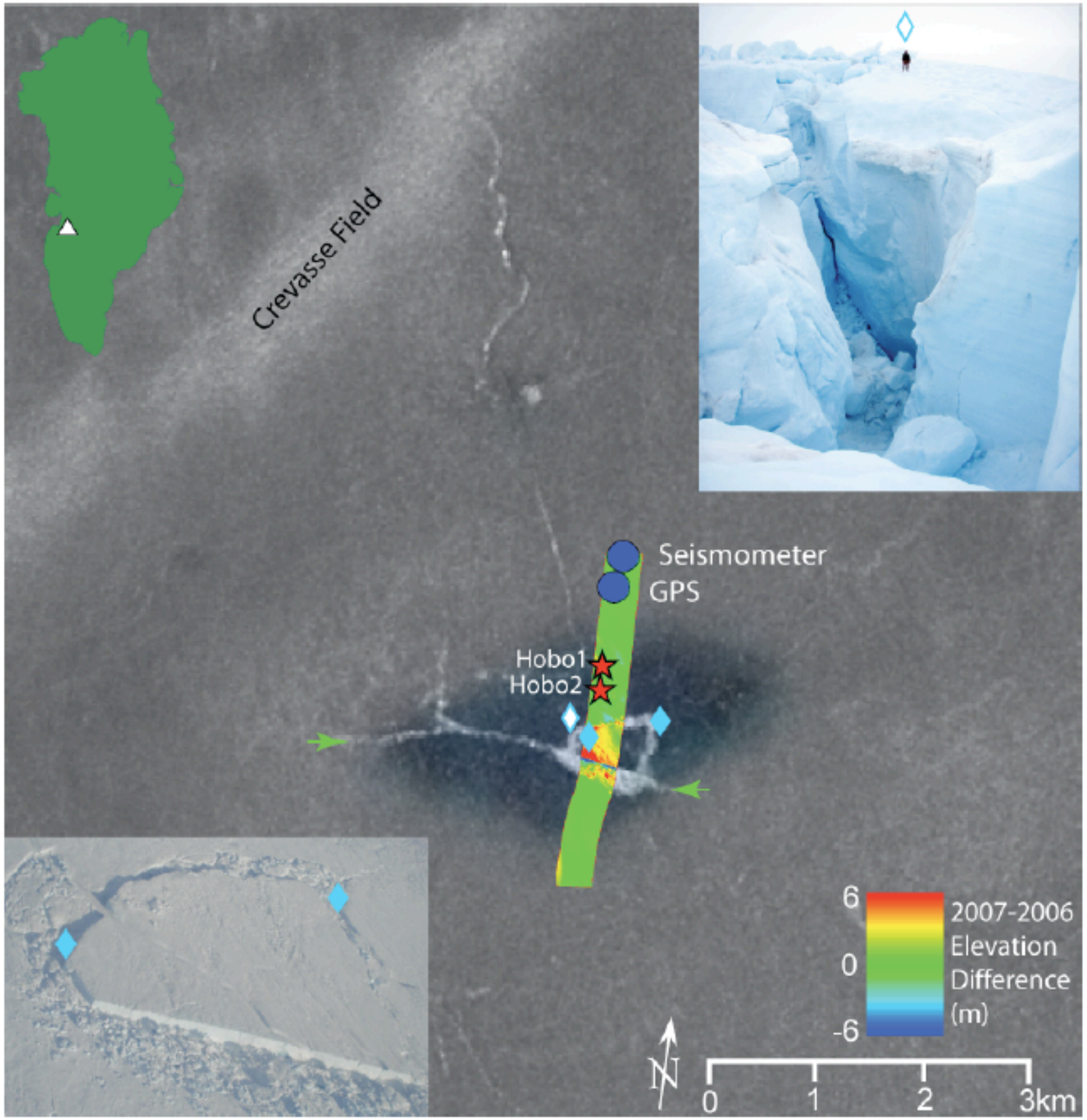

Das et al, science, 2008

Driving Pressure

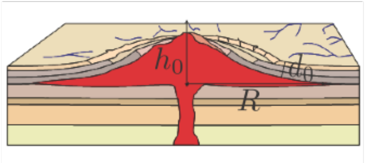

Isoviscous flow
R>>h

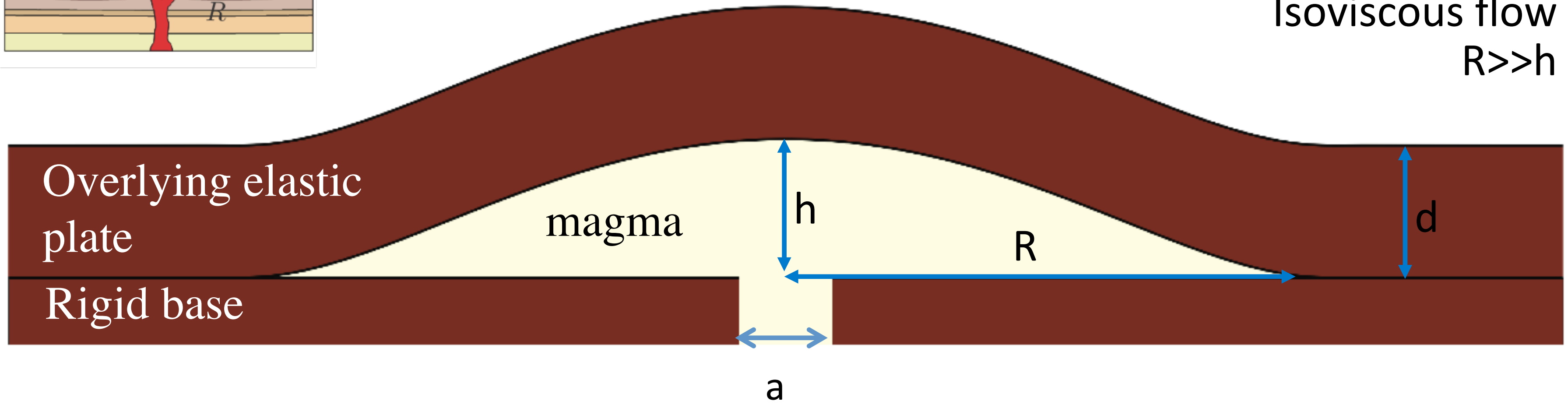

$$P = \underbrace{\rho_m g(h-z)}_{\text{Magma weight}} + \rho_r g d + \underbrace{D\nabla_r^4 h}_{\text{Elastic bending}}$$

Driving Pressure = Magma weight + Elastic bending

$$D = \frac{Ed^3}{12(1-\nu^{*2})}$$

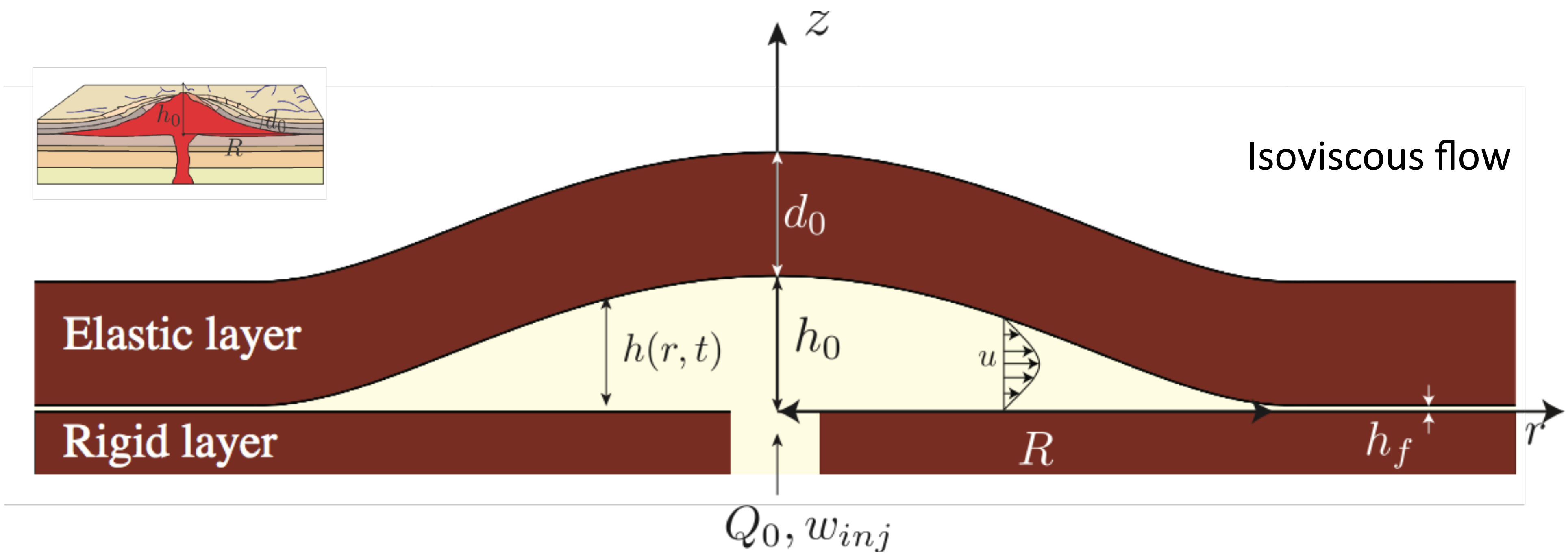

Flexural wavelength

Balance between gravity and bending

$$\Lambda = \left(Ed^3/12(1-\nu^2)\rho_m g\right)^{1/4}$$

Timescale

$$\tau = \frac{\pi\Lambda^2 H}{Q_0}$$

Characteristic thickness

$$H = \left(\frac{12\eta_h Q_0}{\pi\rho_m g}\right)^{1/4}$$

Michaut, 2011
Lister et al, 2013
Hewitt et al, 2015

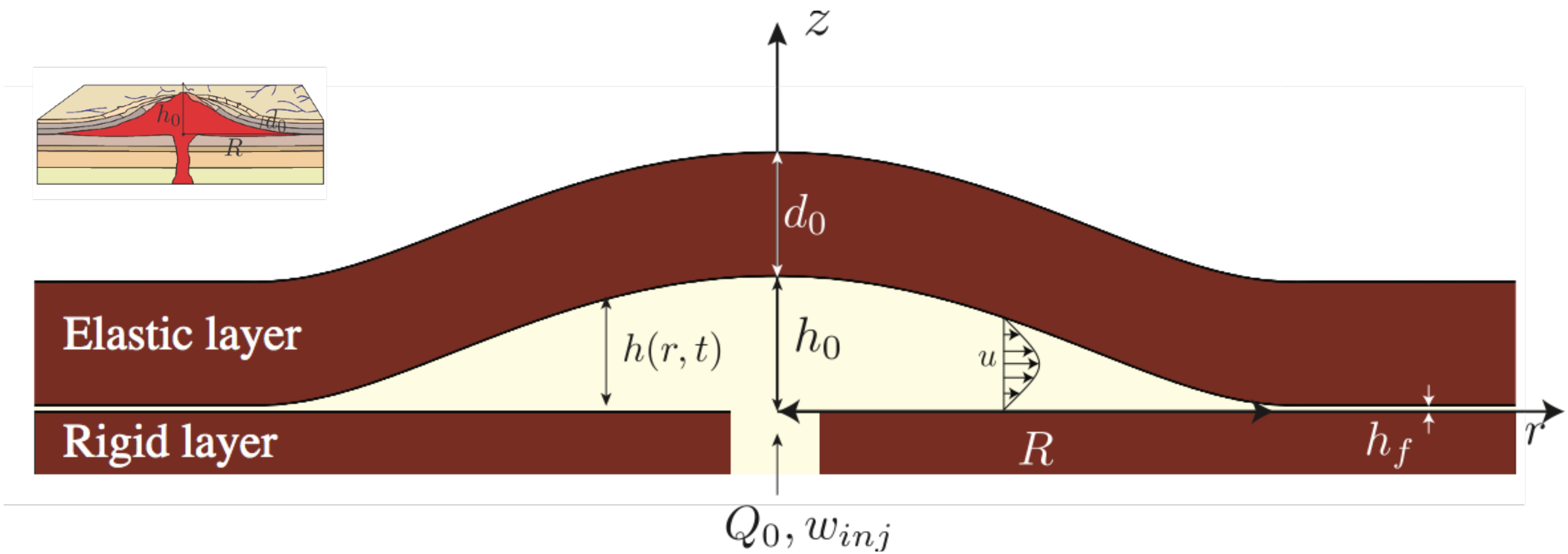

Laminar flow + Lubrication assumptions

$$\frac{\partial h}{\partial t} = \frac{\rho_m g}{12\mu r}\frac{\partial}{\partial r}\left(rh^3\frac{\partial h}{\partial r}\right) + \frac{D}{12\mu r}\frac{\partial}{\partial r}\left(h^3 r\frac{\partial}{\partial r}({\Delta_r}^2 h)\right) + w(r,t)$$

Magma weight

Elastic bending

Michaut, 2011
Lister et al, 2013
Hewitt et al, 2015

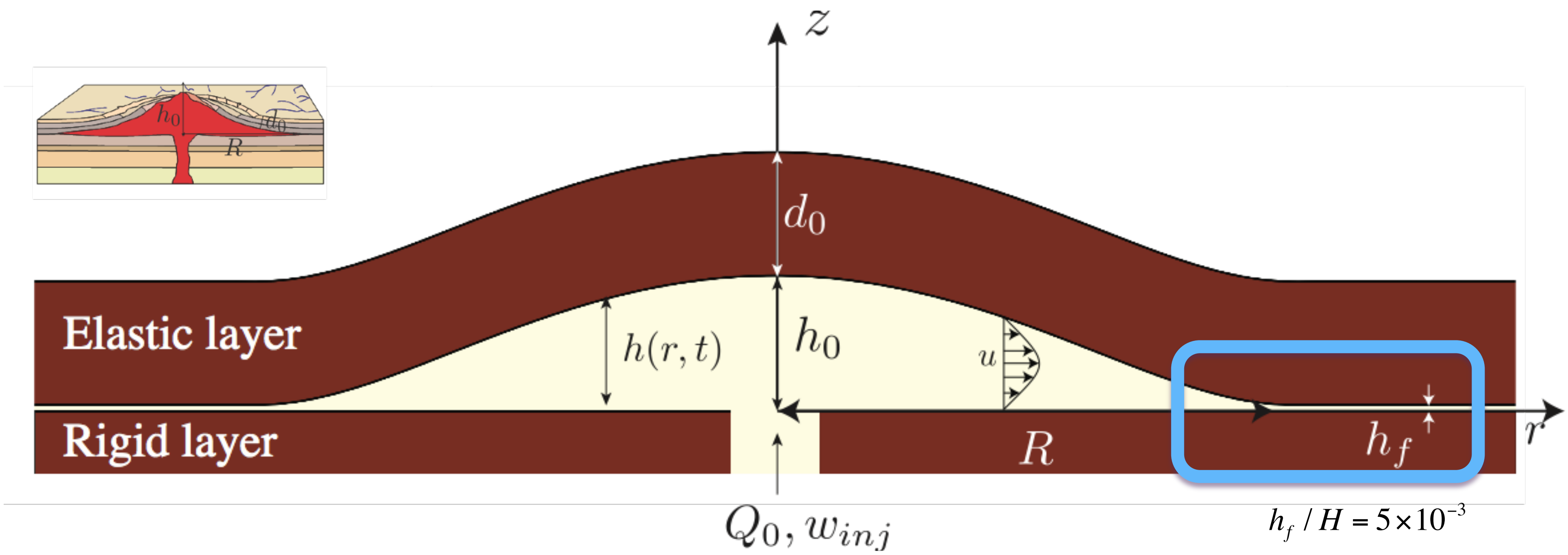

Laminar flow + Lubrication assumptions

$$\frac{\partial h}{\partial t} = \underbrace{\frac{\rho_m g}{12\mu r}\frac{\partial}{\partial r}}_{\text{Magma weight}}\left(r h^3 \frac{\partial h}{\partial r}\right) + \frac{D}{12\mu r}\frac{\partial}{\partial r}\left(\underbrace{h^3 r \frac{\partial}{\partial r}(\Delta_r{}^2 h)}_{\text{Elastic bending}}\right) + w(r,t)$$

Michaut, 2011
Lister et al, 2013
Hewitt et al, 2015

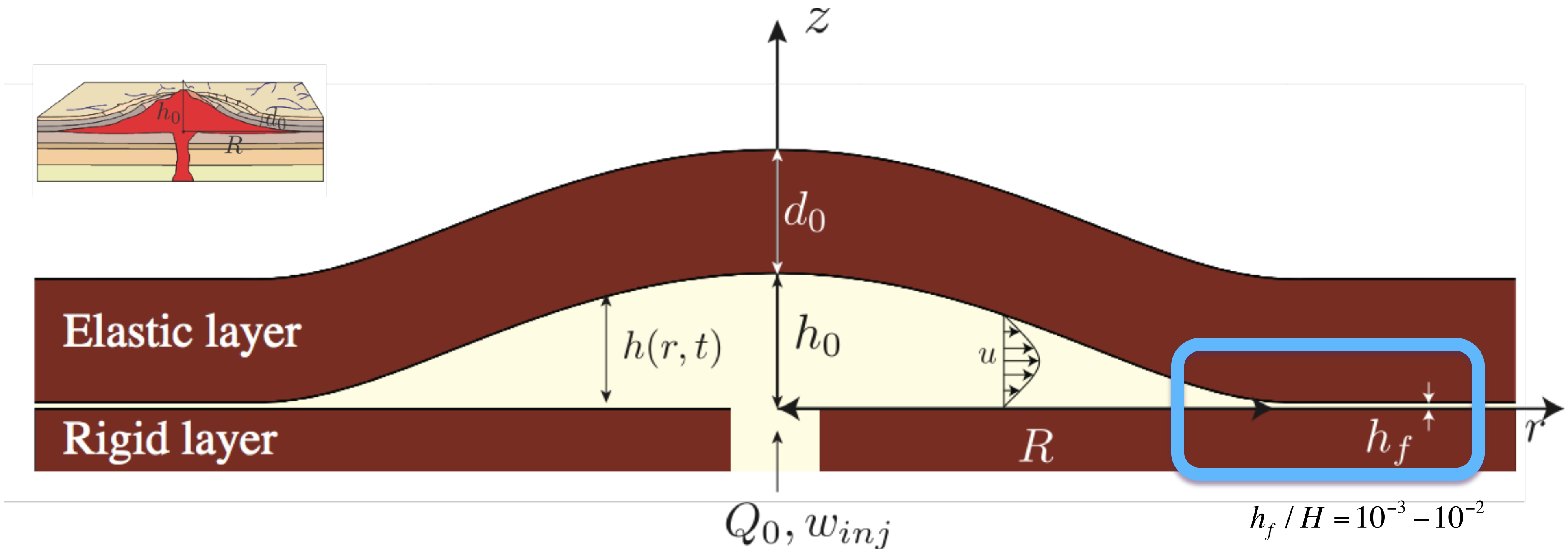

$h_f / H = 10^{-3} - 10^{-2}$

Regularization for the front:
Pre-wetting film of given thickness h_f
or
Gas-filled gap at a given pressure σ

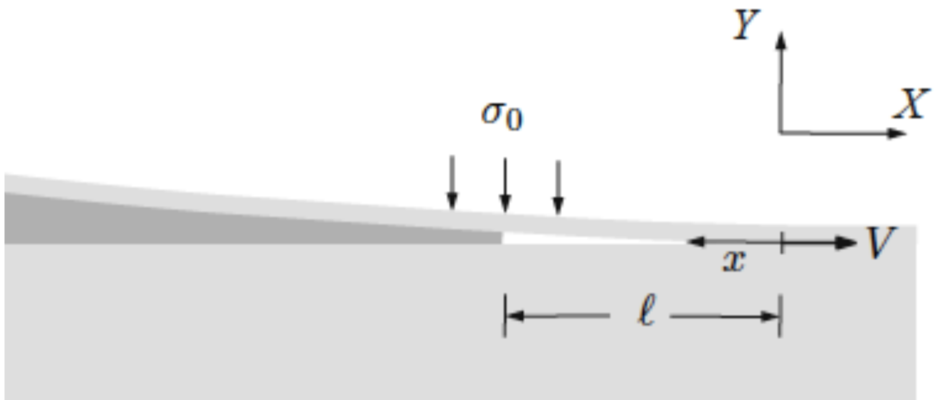

Wang & Detournay, 2018

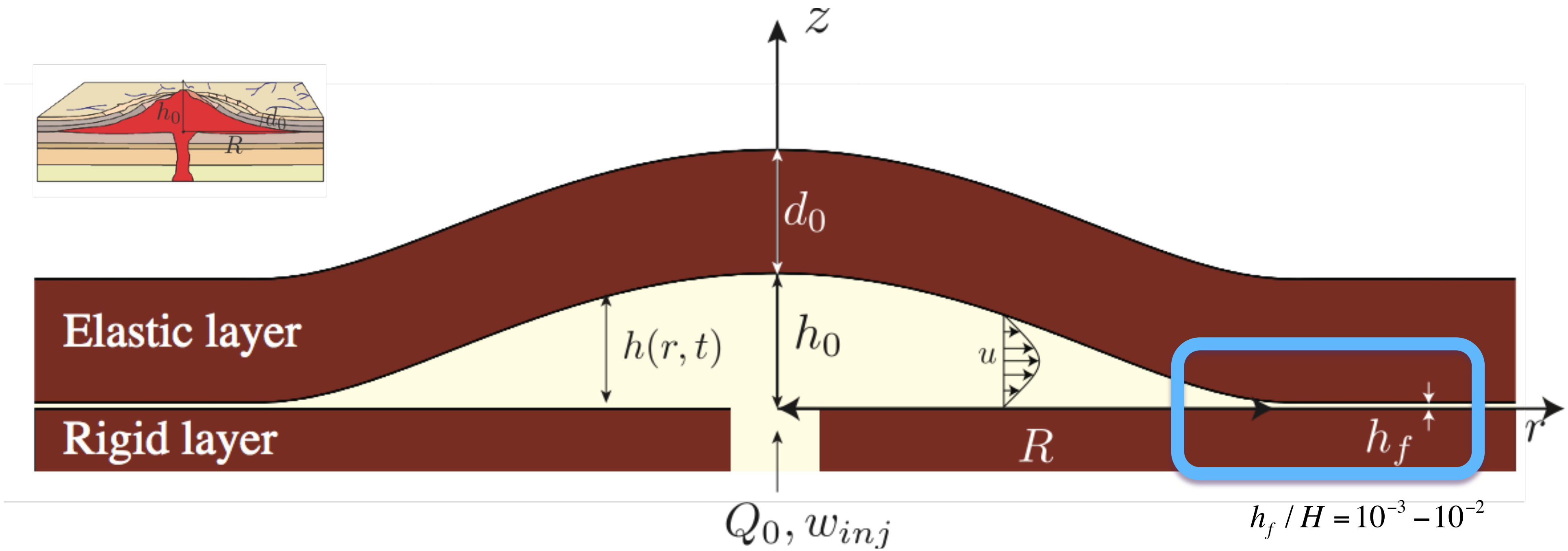

$$\frac{\partial h'}{\partial t'} = \frac{\partial}{\partial r'}\left(r' h'^3 \frac{\partial h'}{\partial r'}\right) + \frac{\partial}{\partial r'}\left(h'^3 r' \frac{\partial}{\partial r'}(\Delta_r'^{\,2} h')\right) + \frac{32}{\gamma^2}\left(\frac{1}{4} - \frac{r'^2}{\gamma^2}\right)$$

$$\gamma = \frac{a}{\Lambda}$$

Michaut, 2011
Lister et al, 2013
Hewitt et al, 2015

Two asymptotic spreading regimes h(t), R(t).

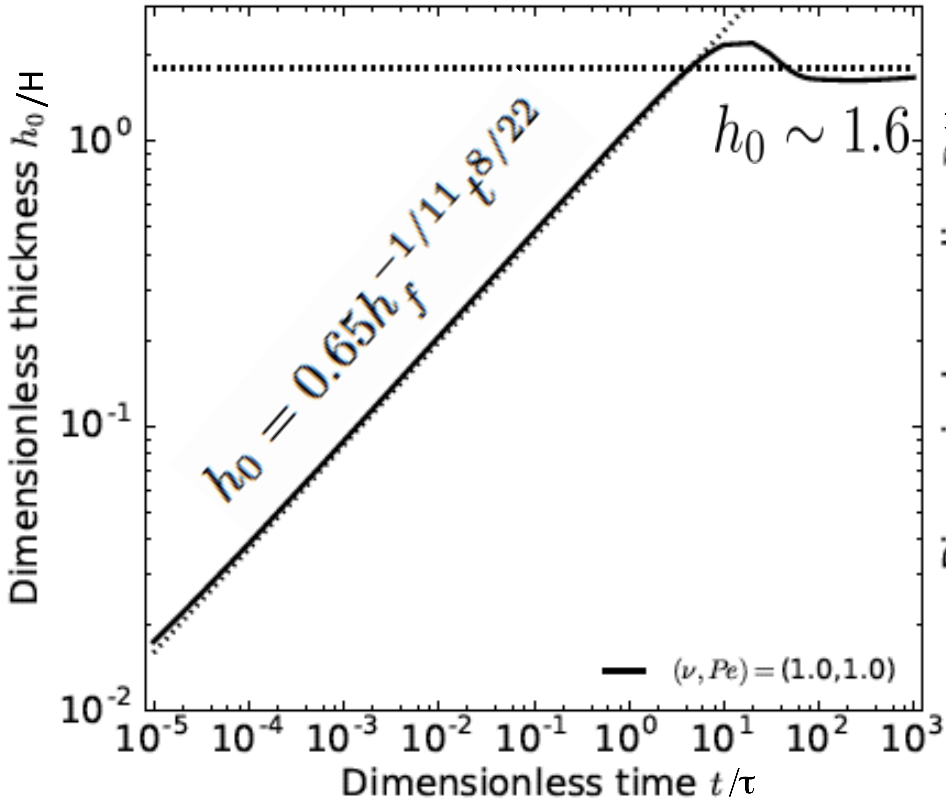

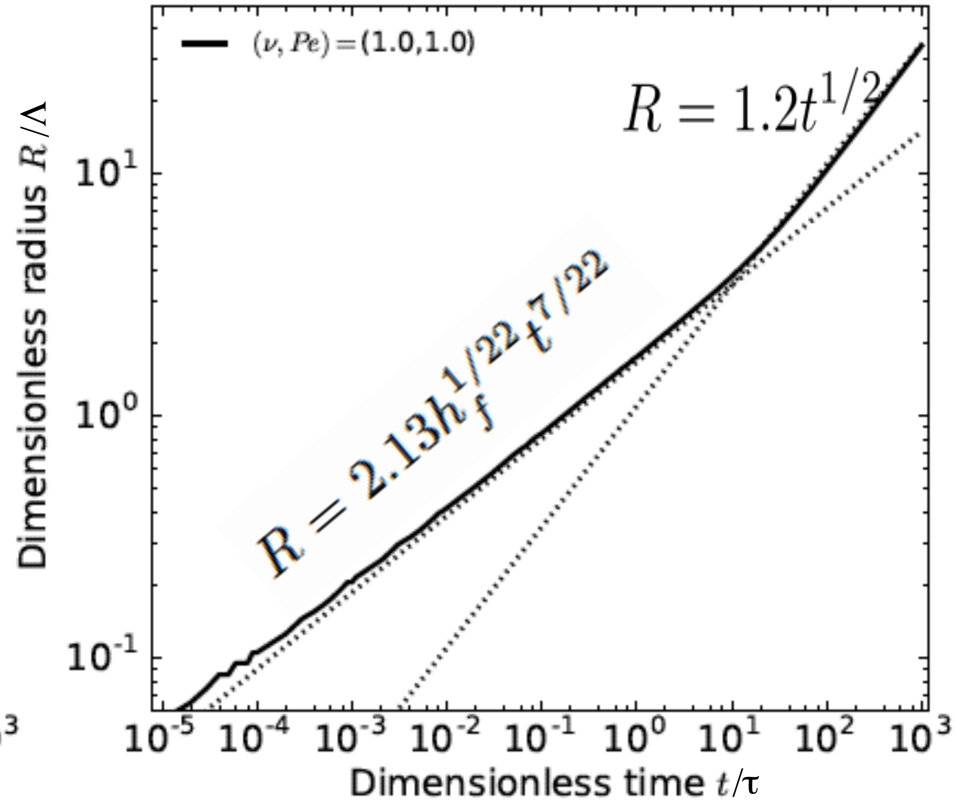

Michaut, 2011
Michaut et al, 2013
Lister et al, 2013
Thorey and Michaut, 2014

Two asymptotic spreading regimes h(t), R(t).

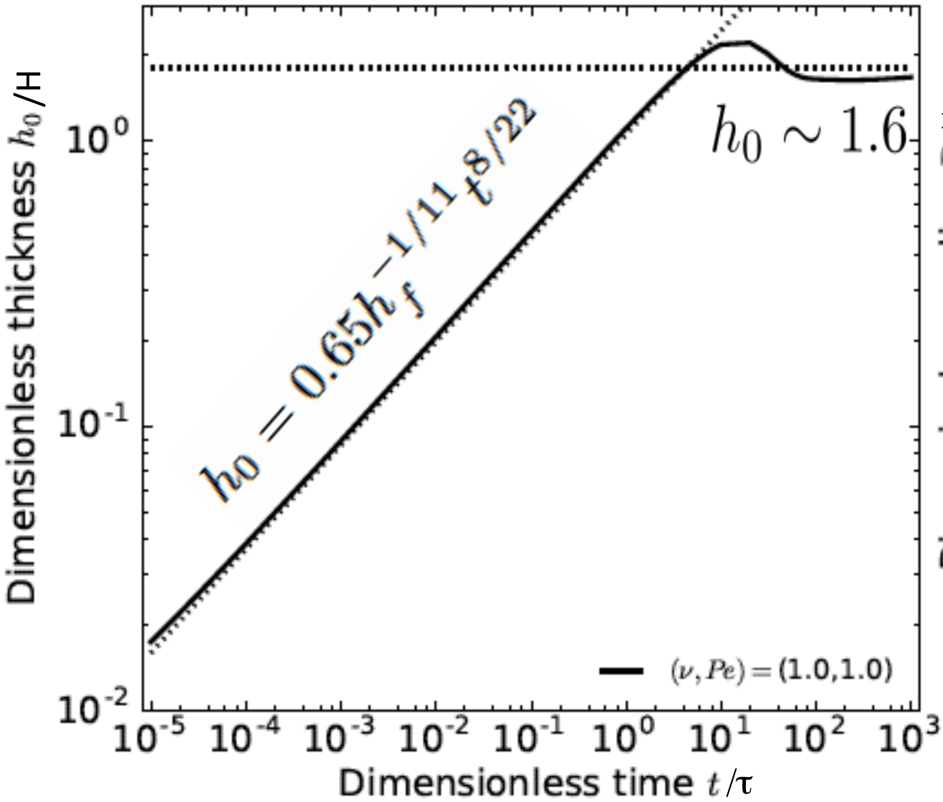

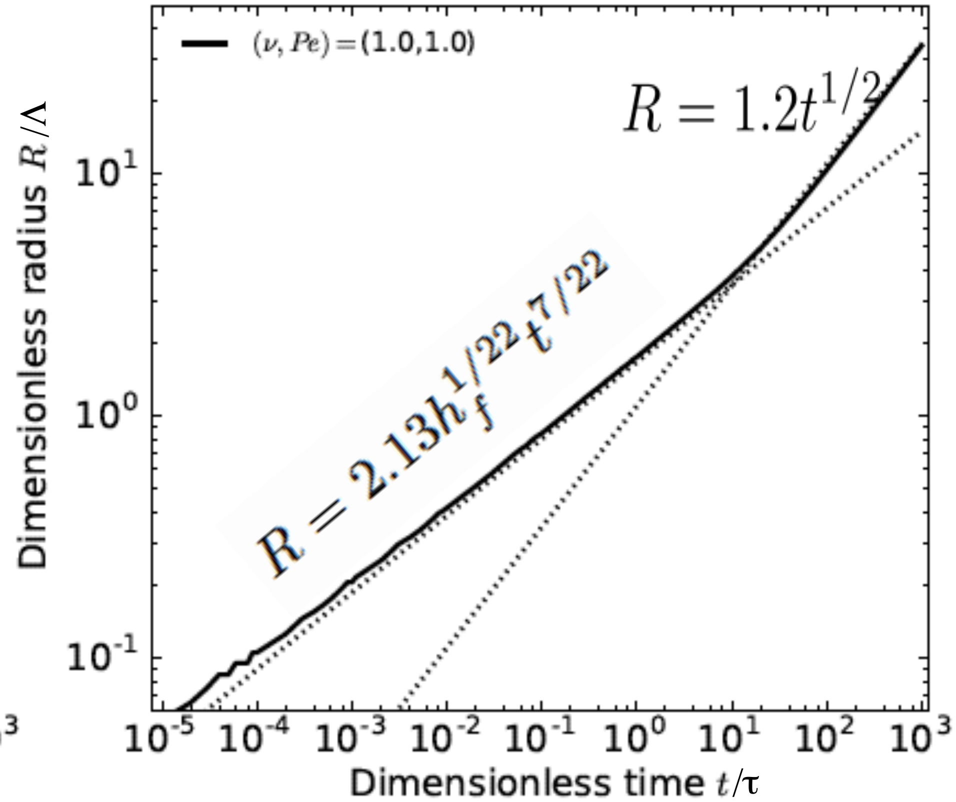

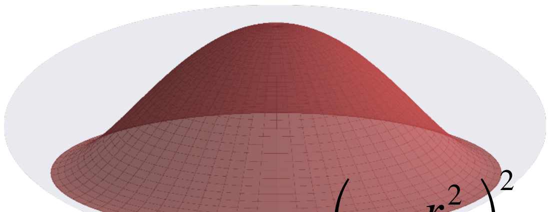

$$h_l(r,t) = h_0(t)\left(1 - \frac{r^2}{R^2}\right)^2$$

Michaut, 2011
Lister et al, 2013

Two asymptotic spreading regimes h(t), R(t).

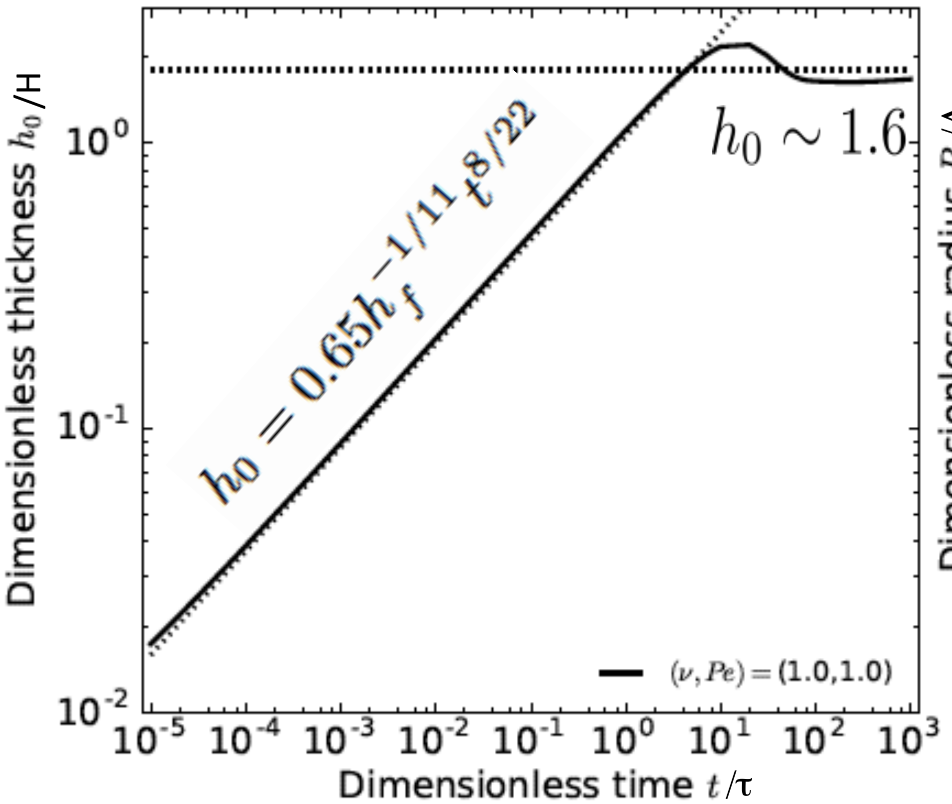

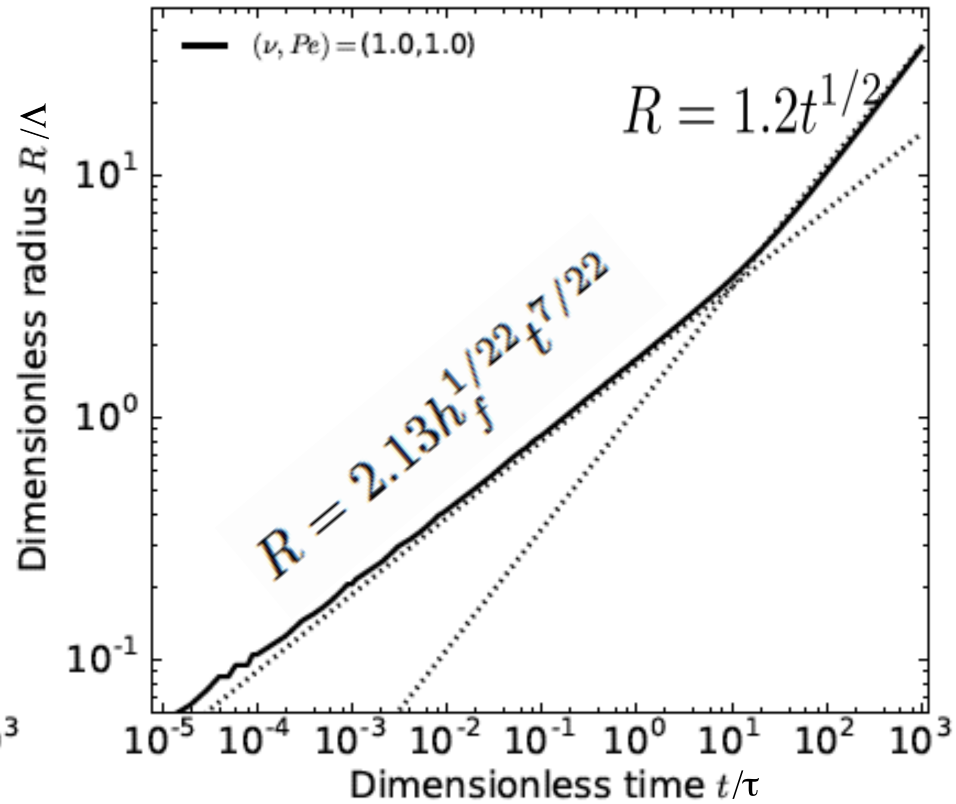

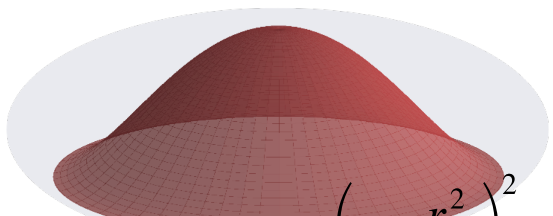

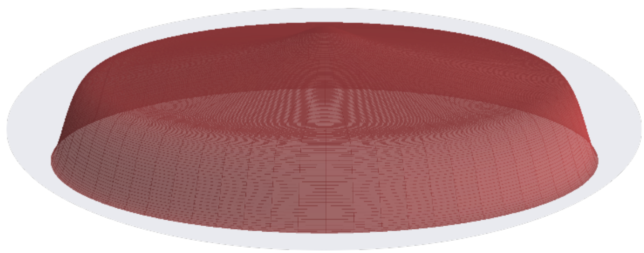

$$h_l(r,t) = h_0(t)\left(1 - \frac{r^2}{R^2}\right)^2$$

Michaut, 2011
Lister et al, 2013

Two asymptotic spreading regimes

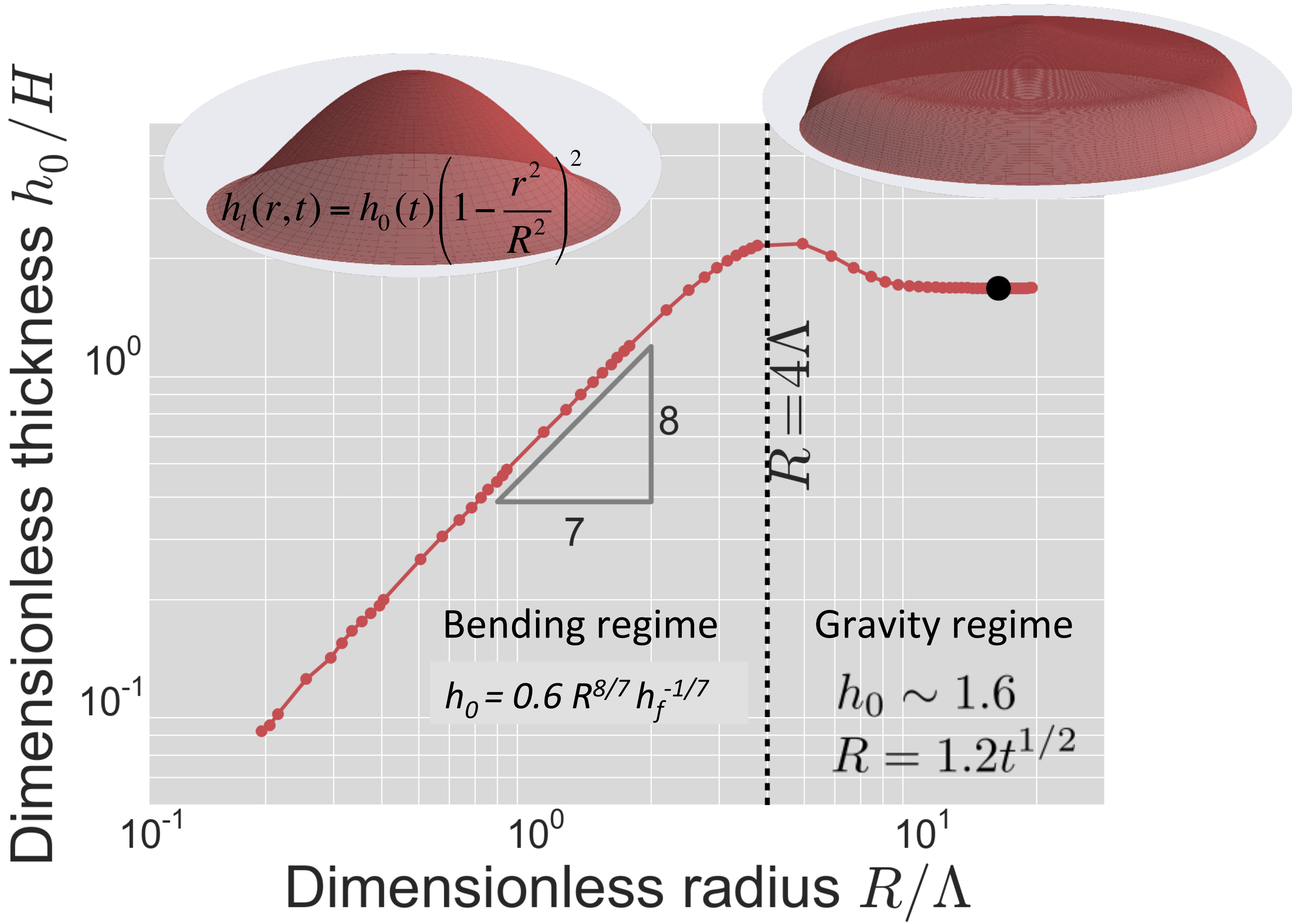

Laccoliths at Elba Island

9 laccoliths between 1.9 and 3.7 km depth

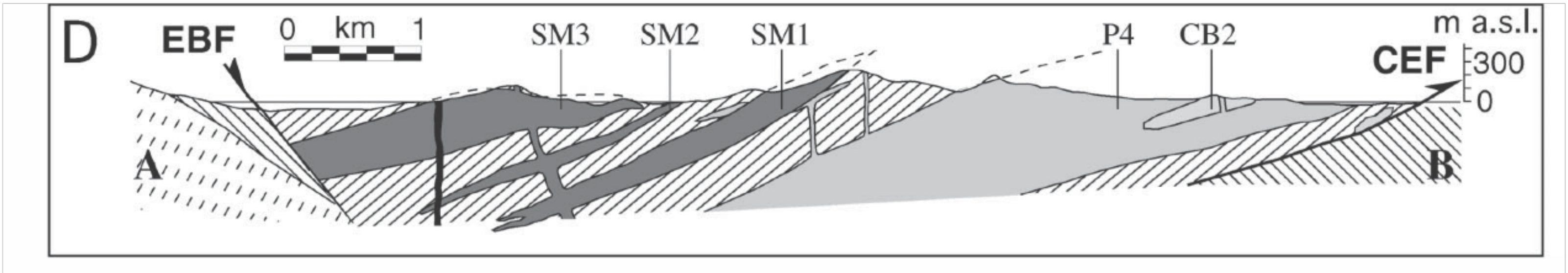

Rocchi et al, 2002

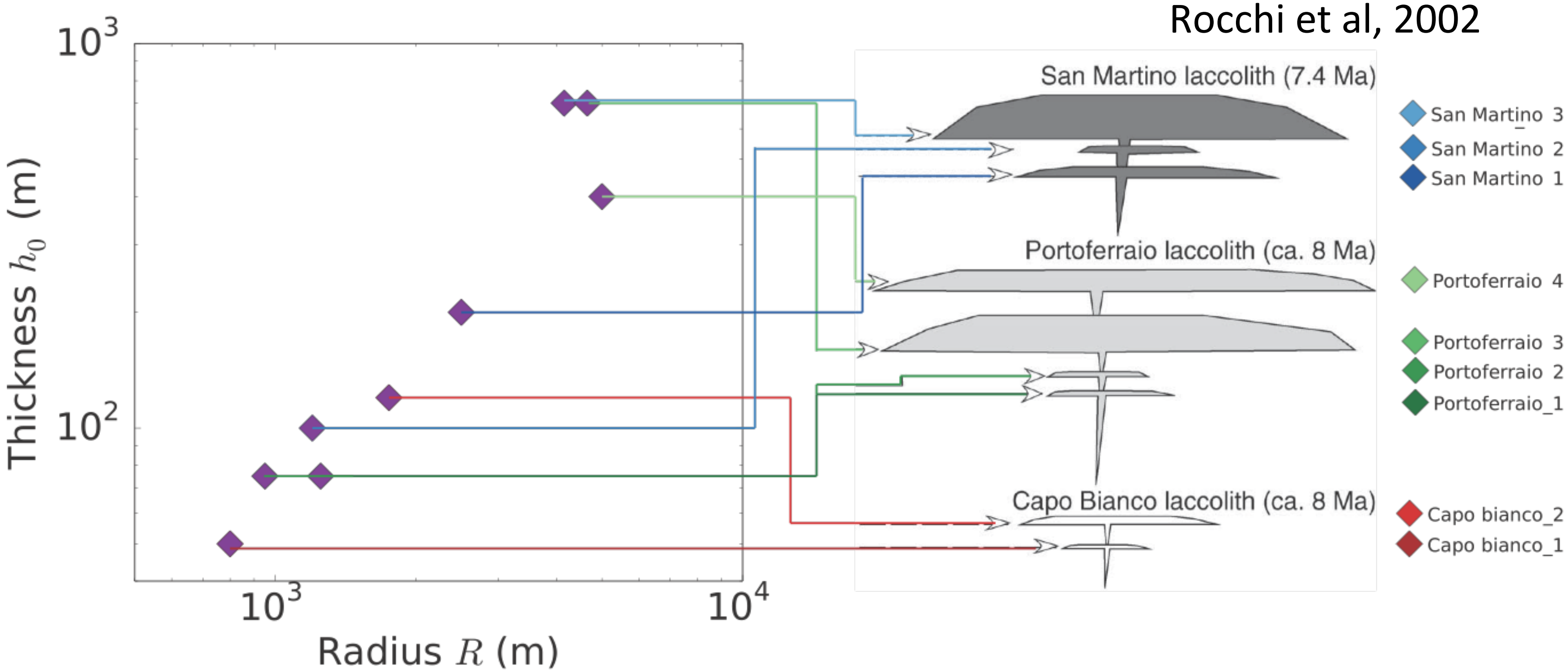

$$\Lambda = (Ed^3/12(1-\nu^2)\rho_m g)^{1/4}$$

$$H = \left(\frac{12\eta_h Q_0}{\pi \rho_m g}\right)^{1/4}$$

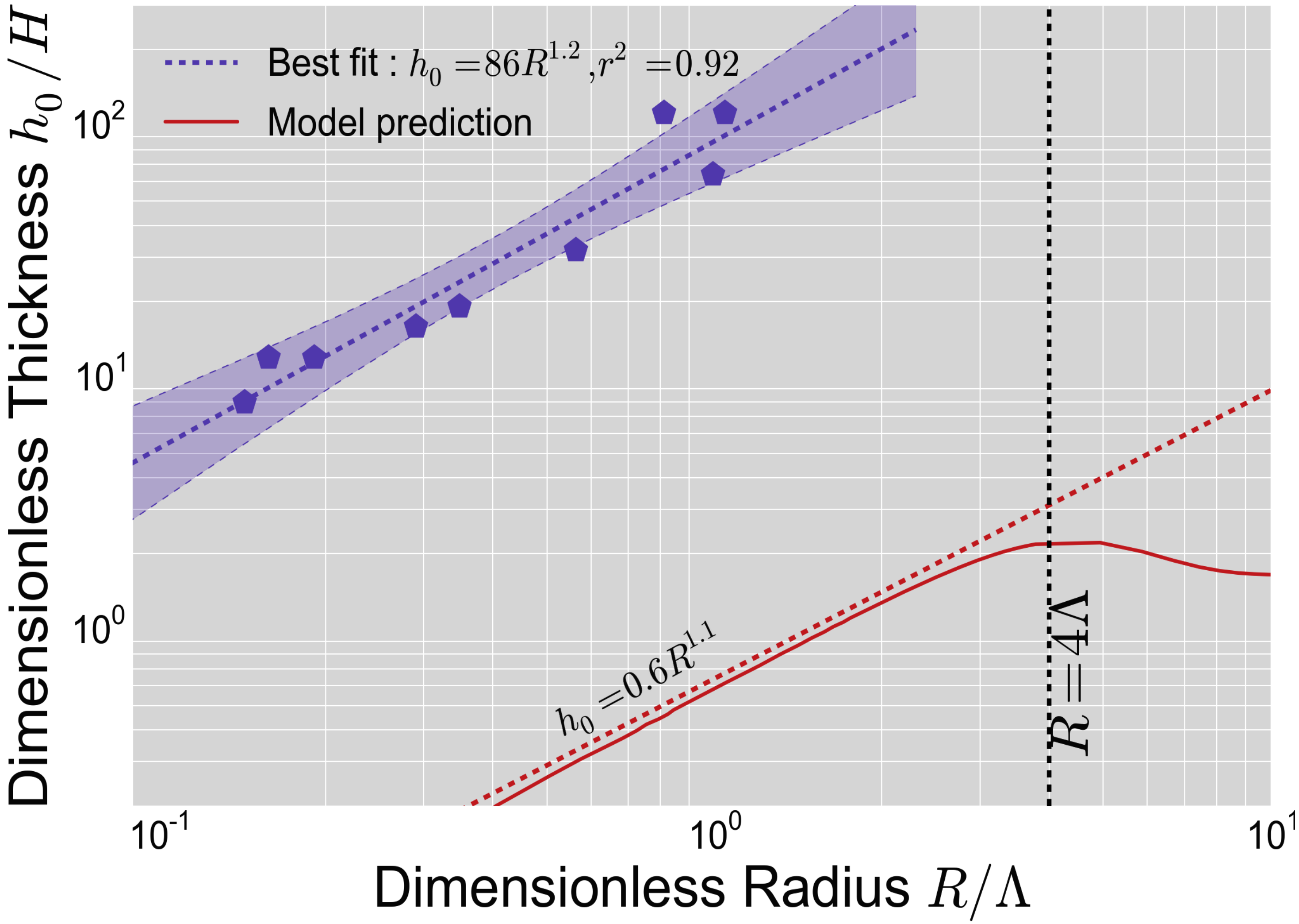

Cooling coupled to the flow

Temperature-dependent viscosity

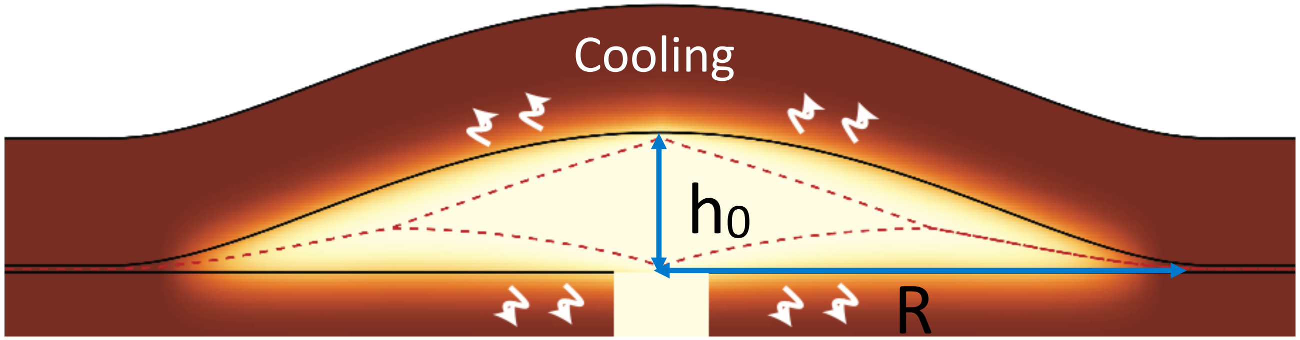

$$\nu = \frac{\eta_{\text{hot}}}{\eta_{\text{cold}}}$$

$$Pe = \frac{HQ_0}{\pi\kappa\Lambda^2}$$

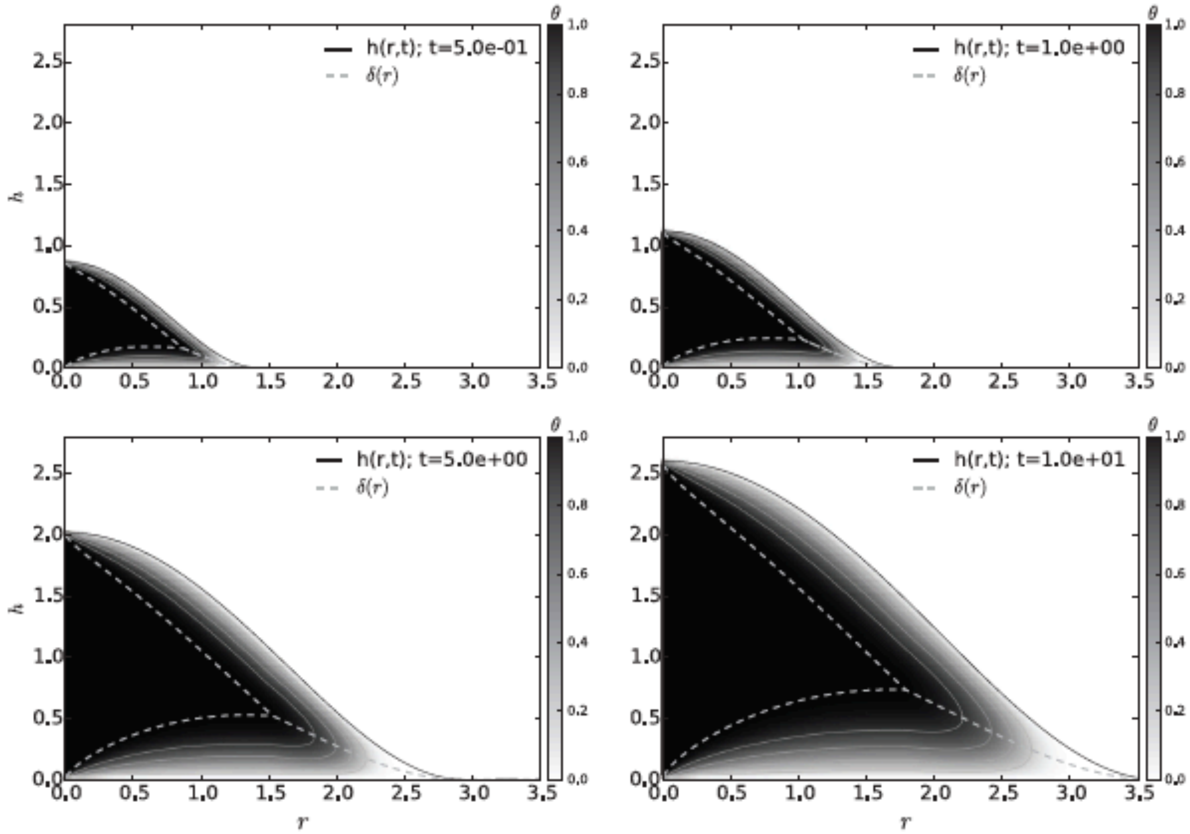

Cooling

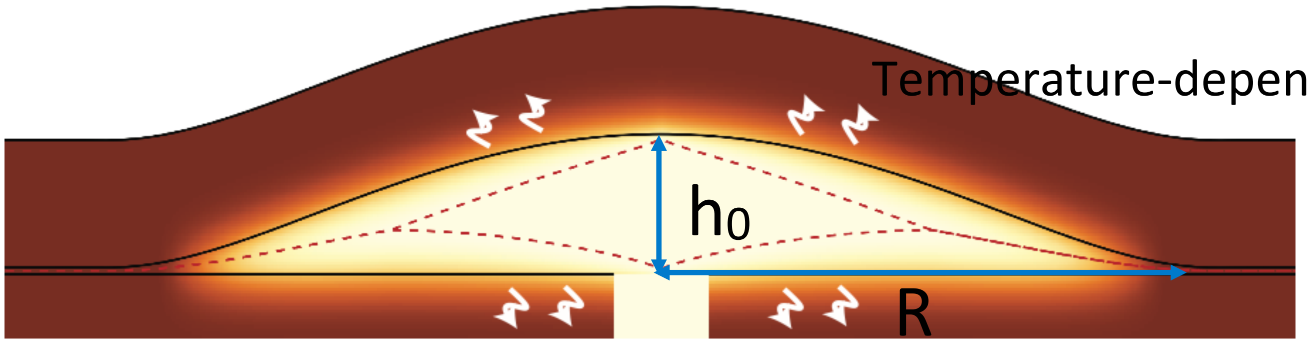

Temperature-dependent viscosity

$$\nu = \frac{\eta_{\mathrm{hot}}}{\eta_{\mathrm{cold}}}$$

$$Pe = \frac{HQ_0}{\pi \kappa \Lambda^2}$$

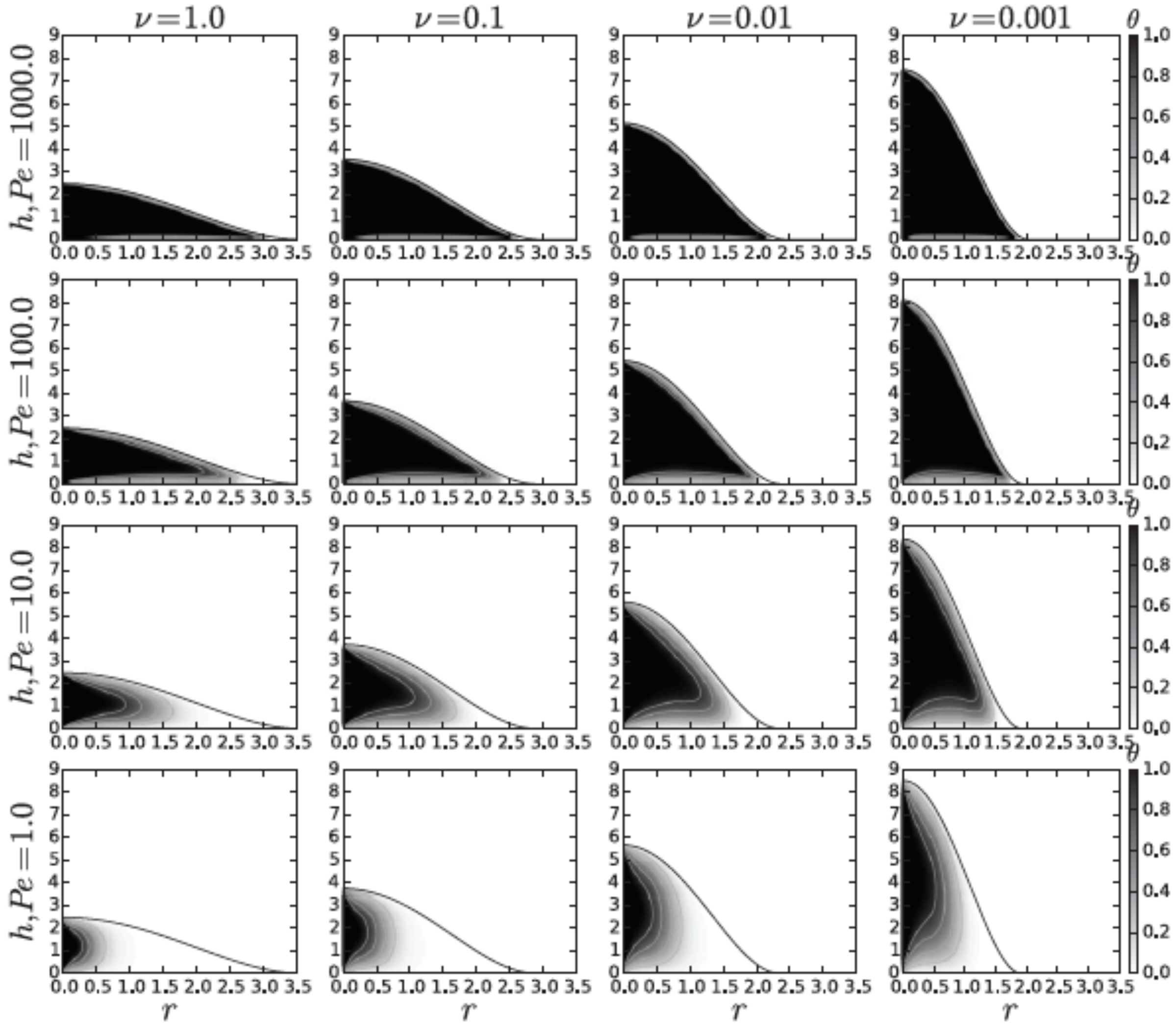

Cooling in the bending regime

Temperature-dependent viscosity

$$\nu = \frac{\eta_{\text{hot}}}{\eta_{\text{cold}}}$$

$$Pe = \frac{HQ_0}{\pi\kappa\Lambda^2}$$

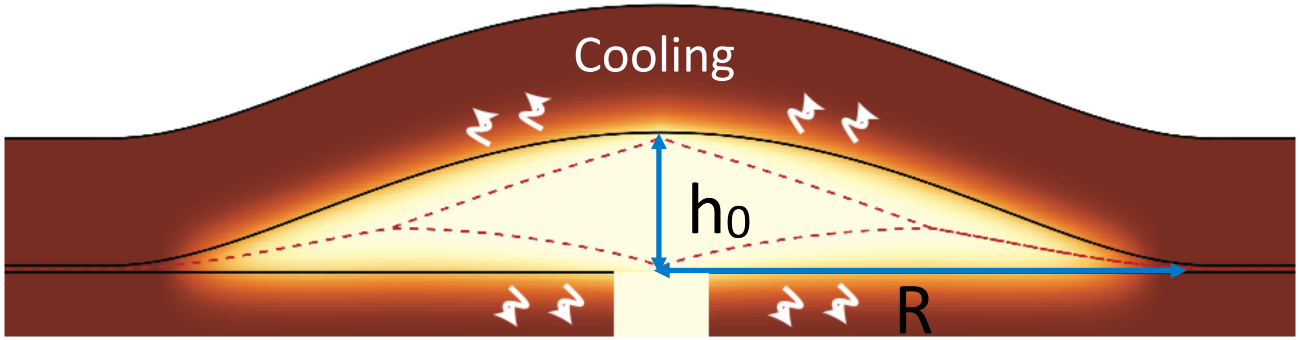

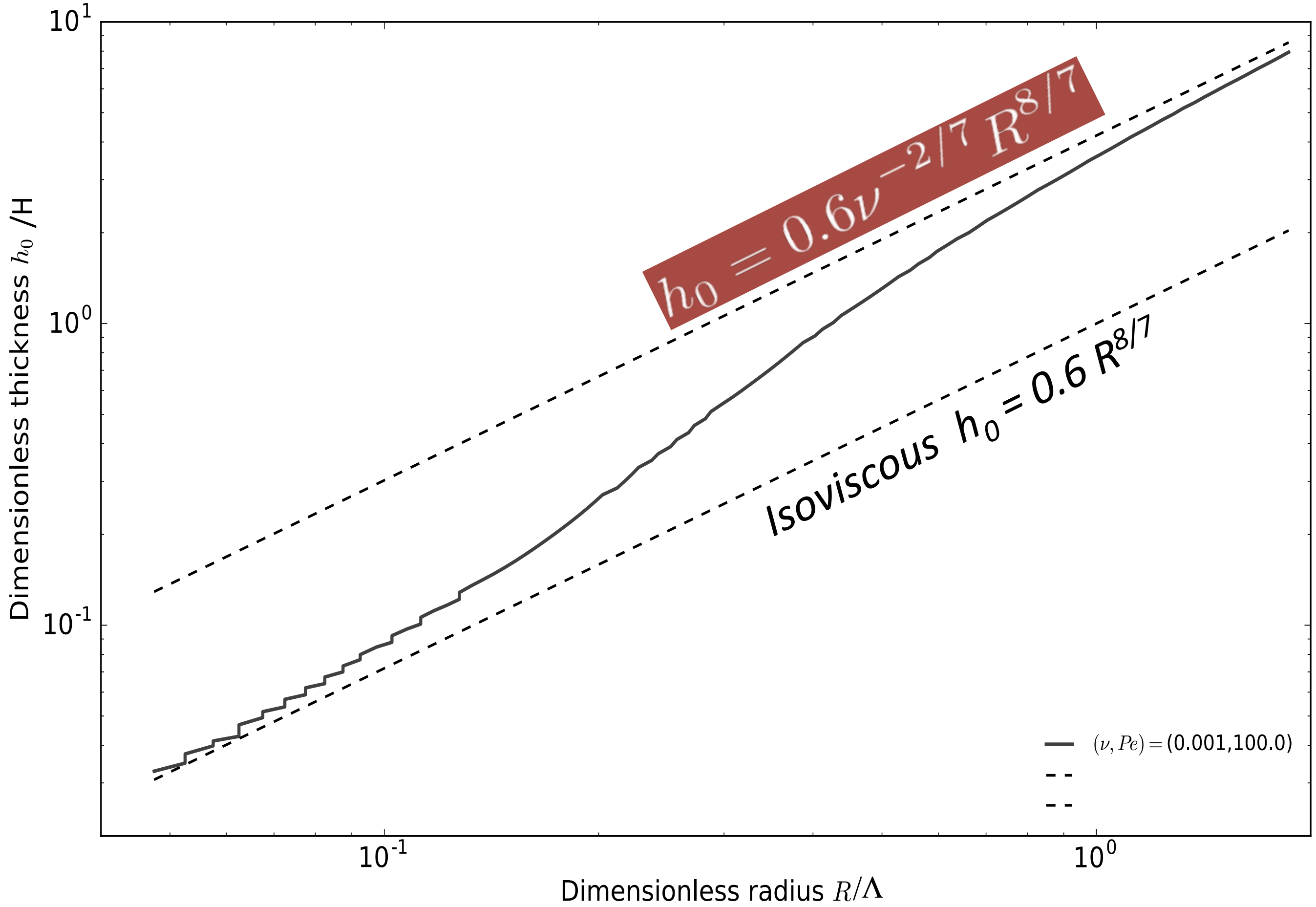

Cooling in the bending regime

Temperature-dependent viscosity

$$\nu = \frac{\eta_{\rm hot}}{\eta_{\rm cold}}$$

$$Pe = \frac{HQ_0}{\pi\kappa\Lambda^2}$$

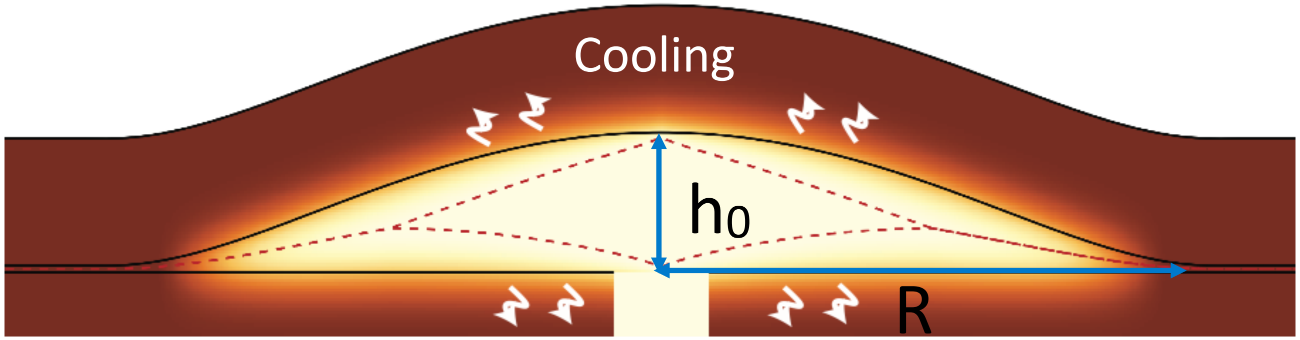

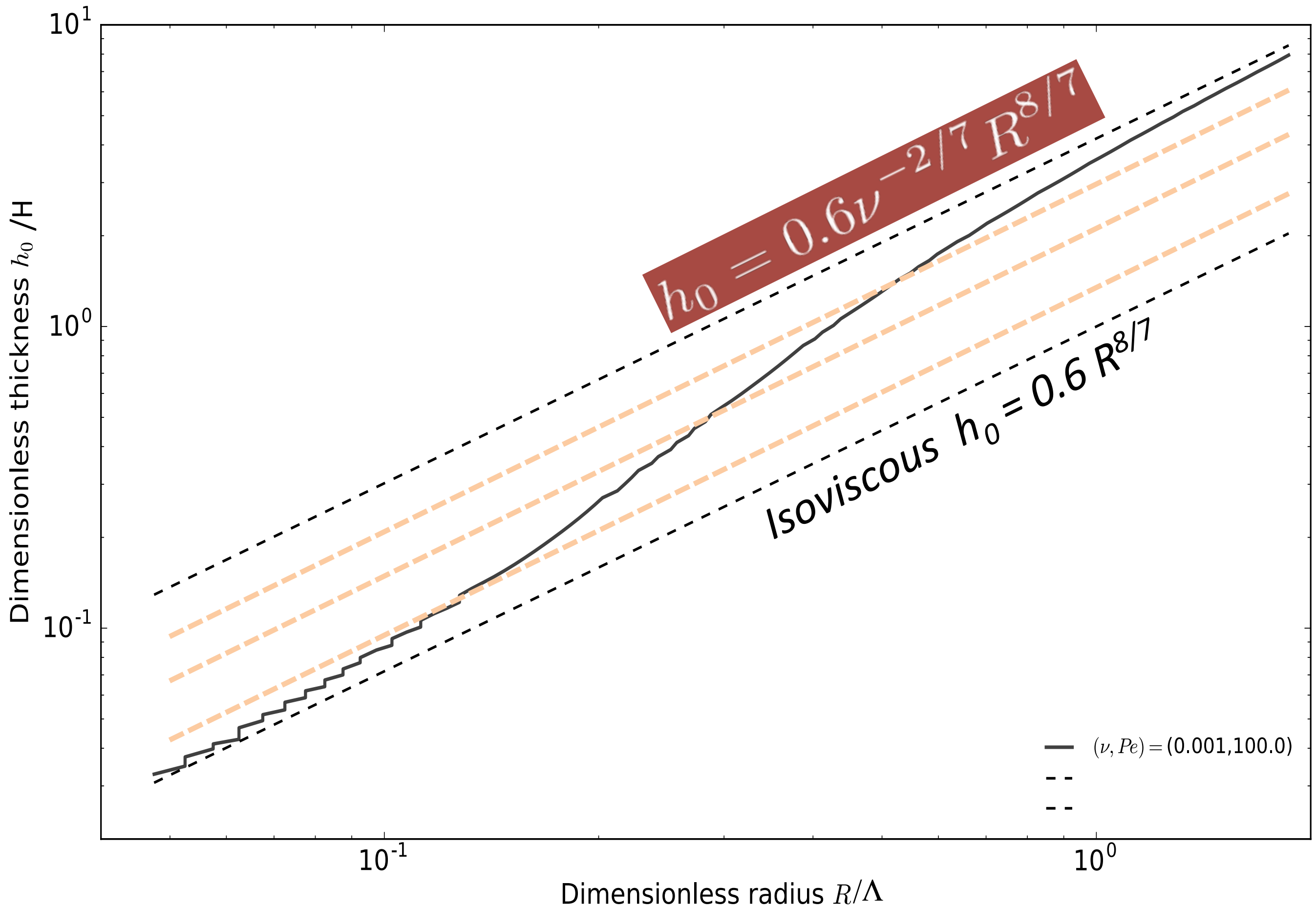

Cooling in the bending regime

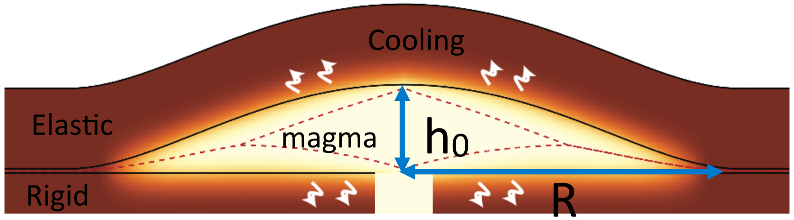

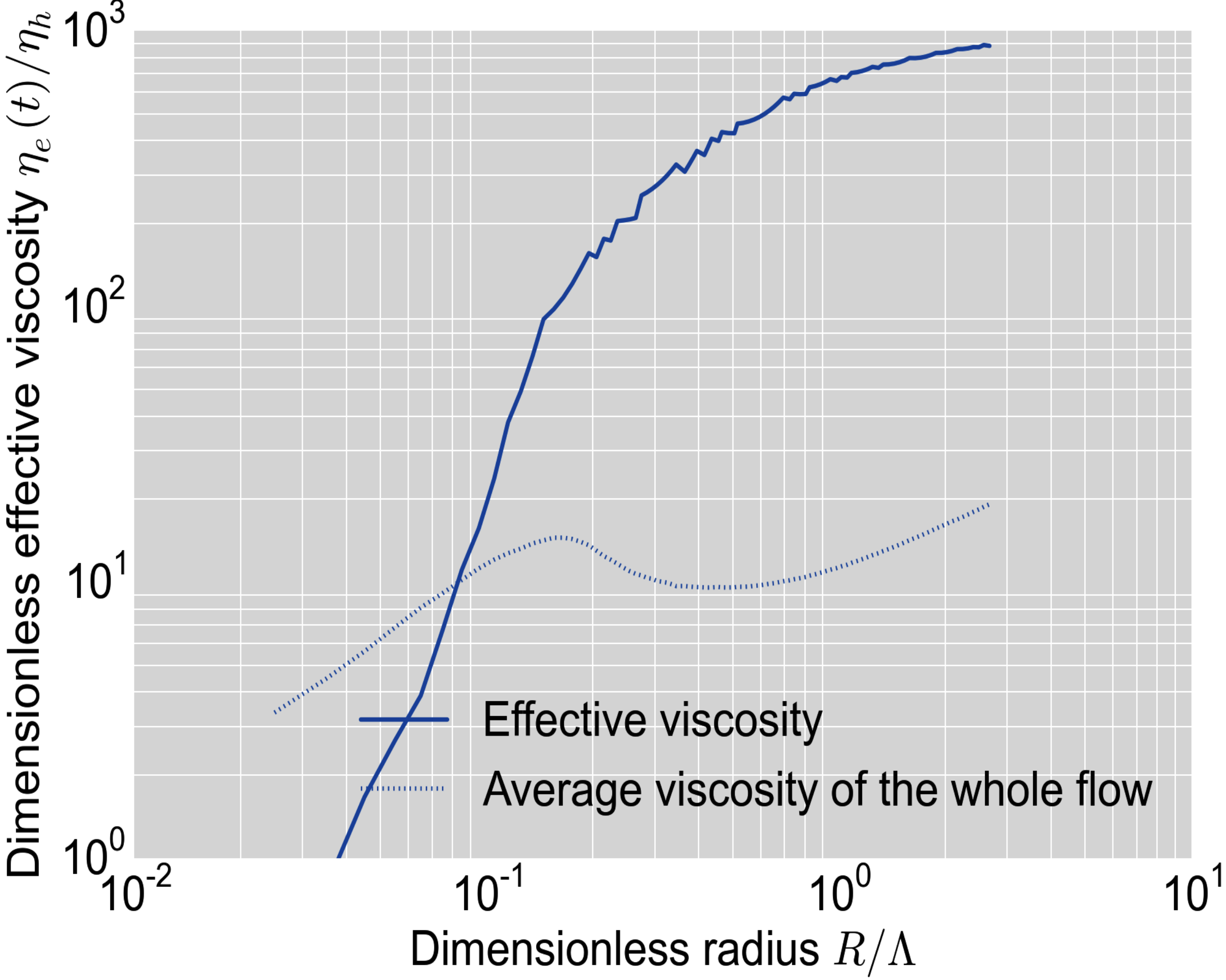

Cooling in the bending regime

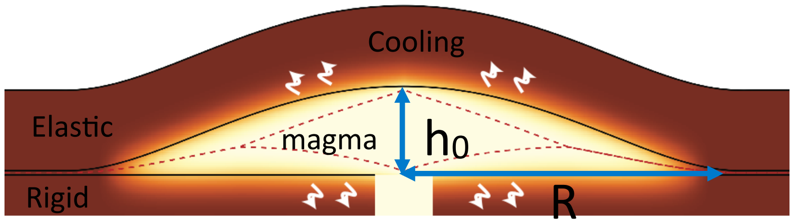

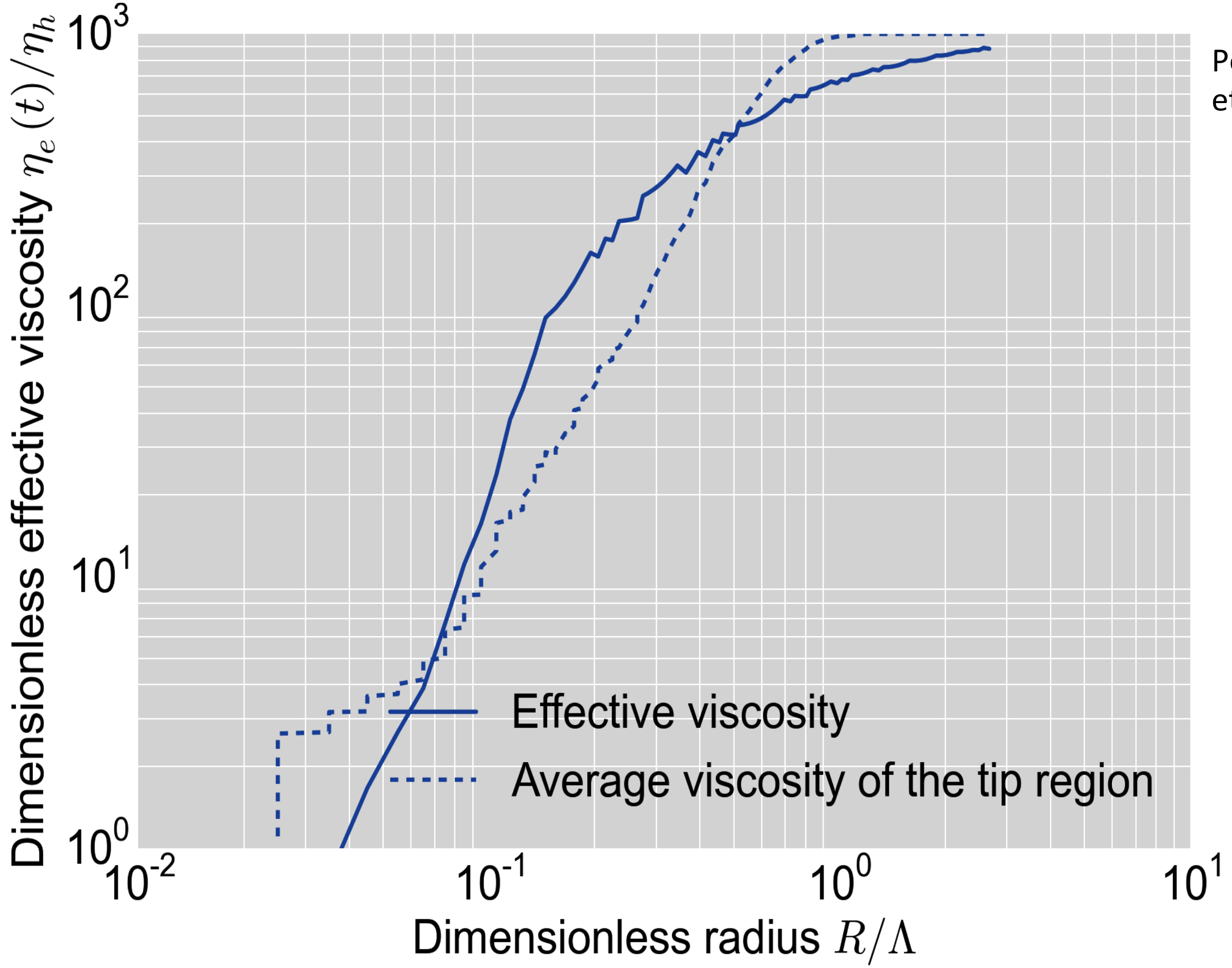

Peeling length scale (Lister et al, 2013)

$$L_P = \left(\frac{D h_f^3}{12 \eta_e dR/dt} \right)^{1/5}$$

- ➢ Flow propagation controlled by the viscosity of a small region at the tip

Thorey & Michaut, JFM 2016

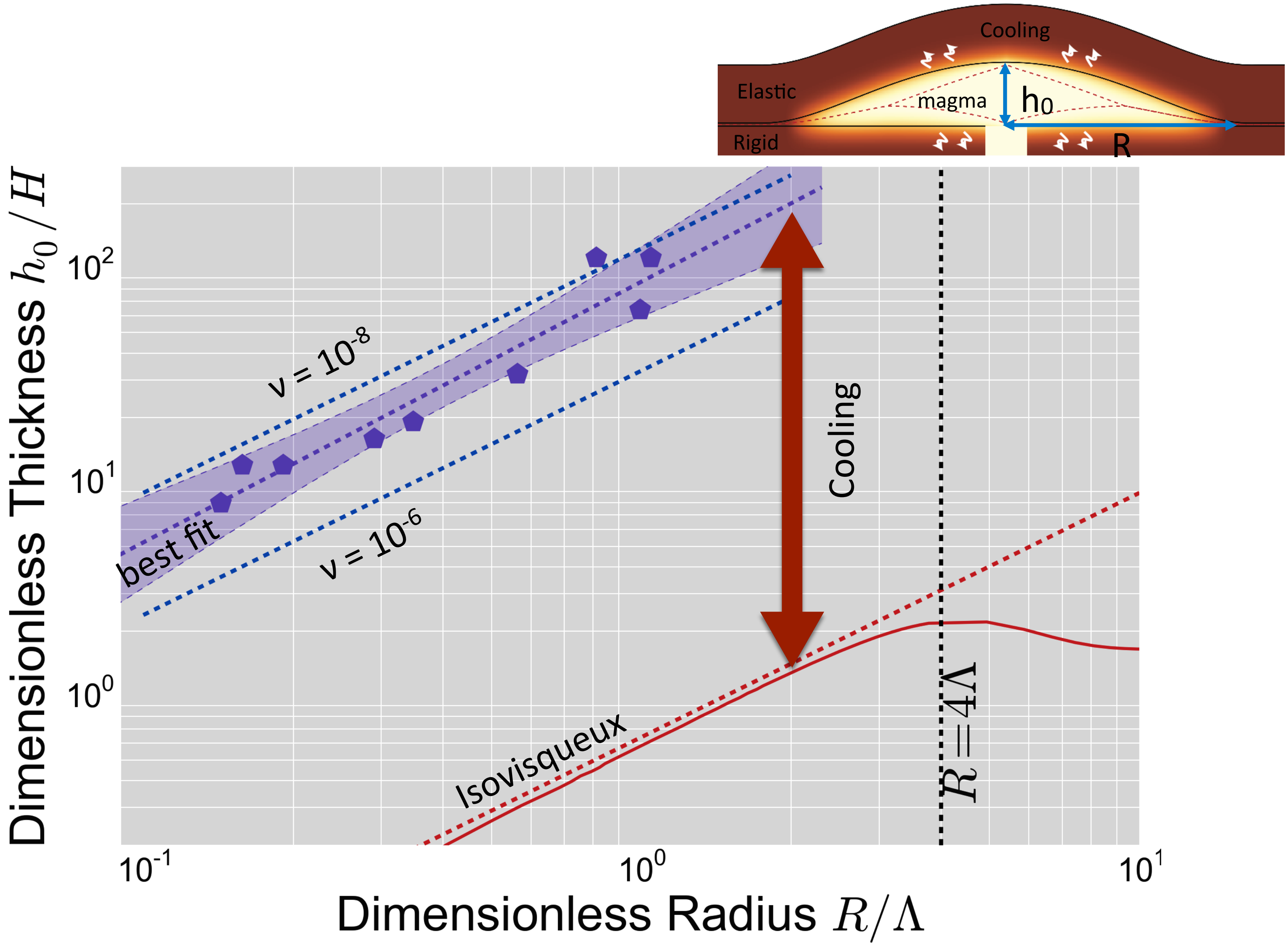
Cooling
Elastic
magma
h_0
Rigid
R
Dimensionless Thickness h_0/H
10^2
10^1
10^0
$\nu = 10^{-8}$
$\nu = 10^{-6}$
best fit
Cooling
Isovisqueux
$R=4\Lambda$
10^{-1}
10^0
10^1
Dimensionless Radius R/Λ

Lunar floor-fractured craters (FFCs)

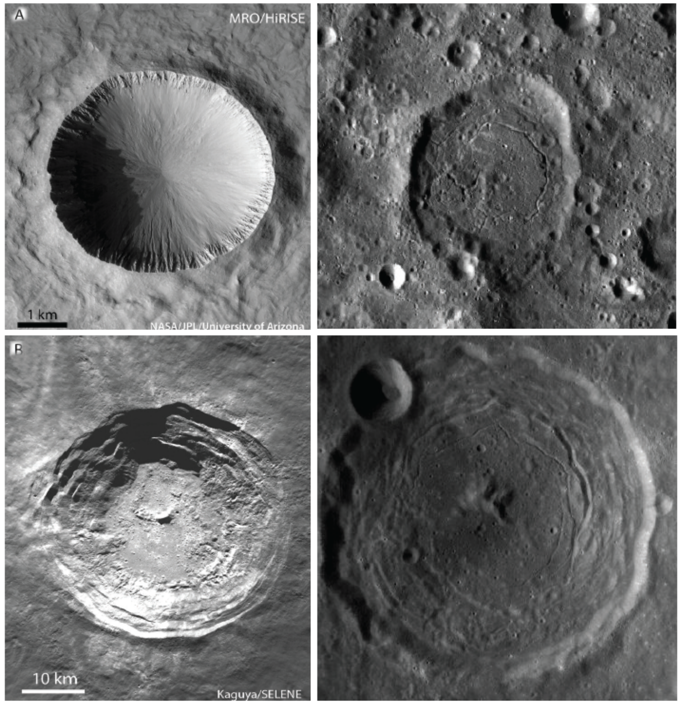

Regular impact craters

Floor-fractured craters
~10 to 100 km radius
Number : ~200

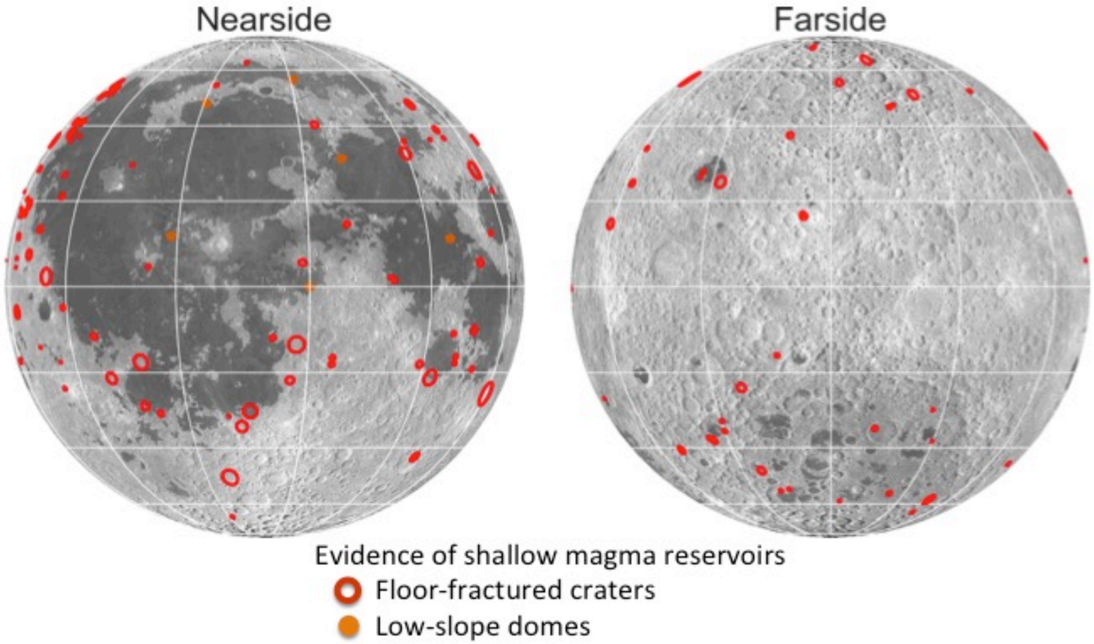

Flow below a crater

Crater-centered intrusion – floor-fractured craters

LROC WAC - Oblique Komarov FFC
~80 km in diameter

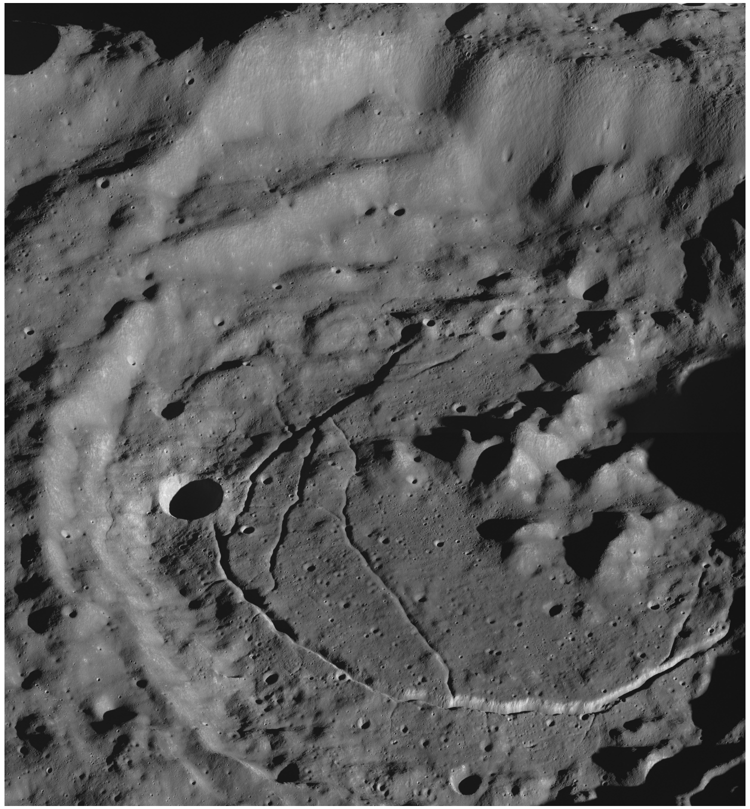

LROC NAC - Oblique Karpinskiy FFC
~90 km in diameter

NASA/GSFC/Arizona State University

Two types of floor appearance at lunar floor-fractured craters

Uplifted convex floor

FFC Briggs, 37 km in diameter

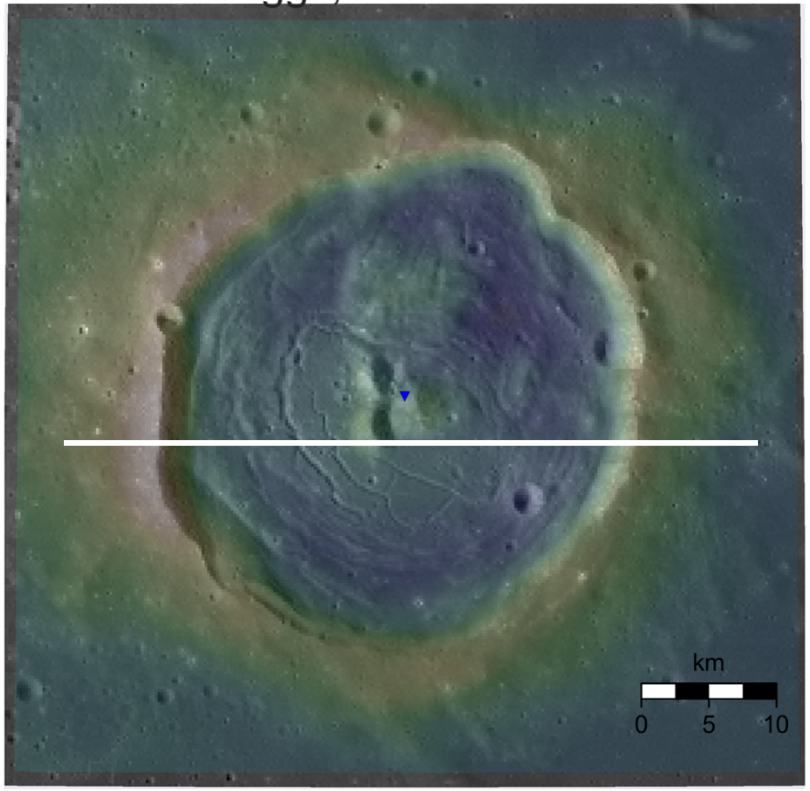

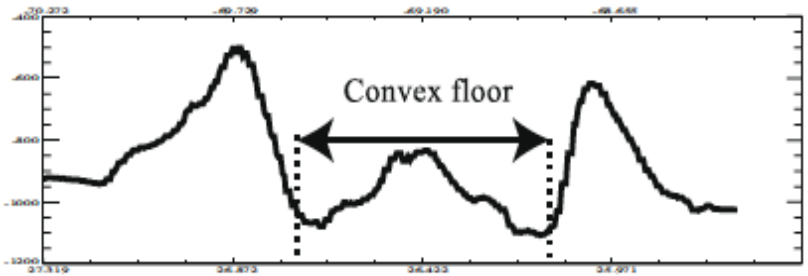

Uplifted flat floor with a circular moat

FFC Warner, 35 km in diameter

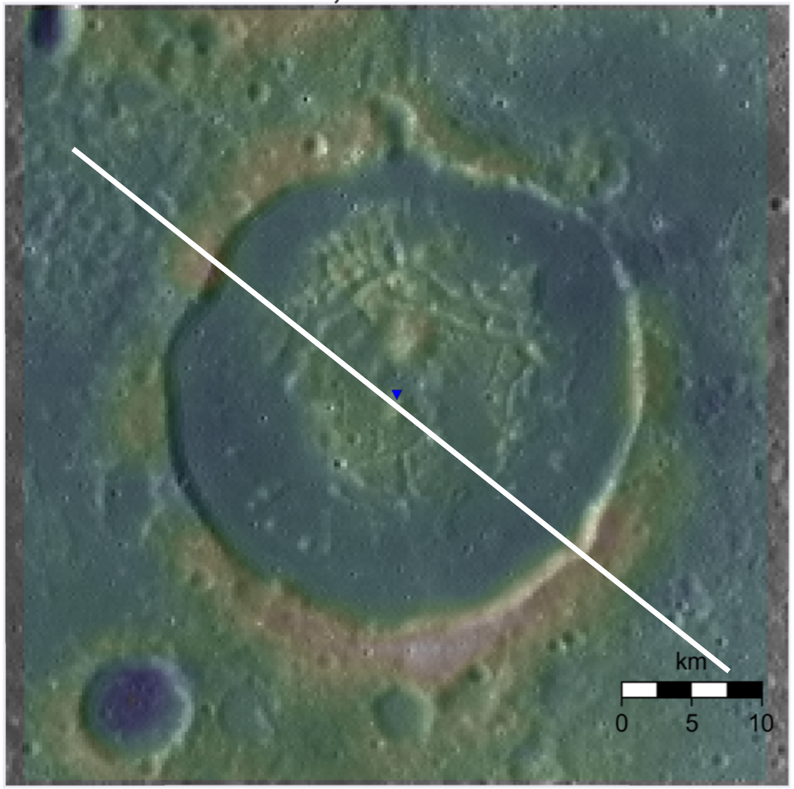

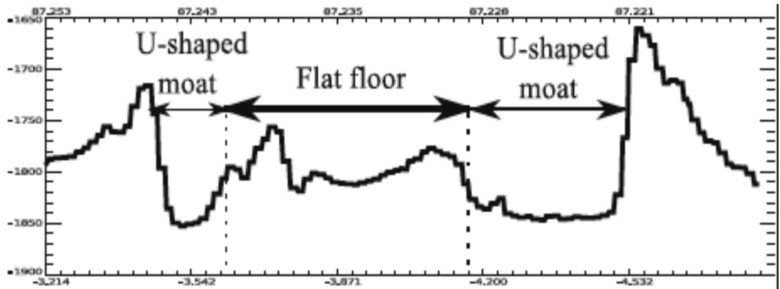

Thorey & Michaut, 2014

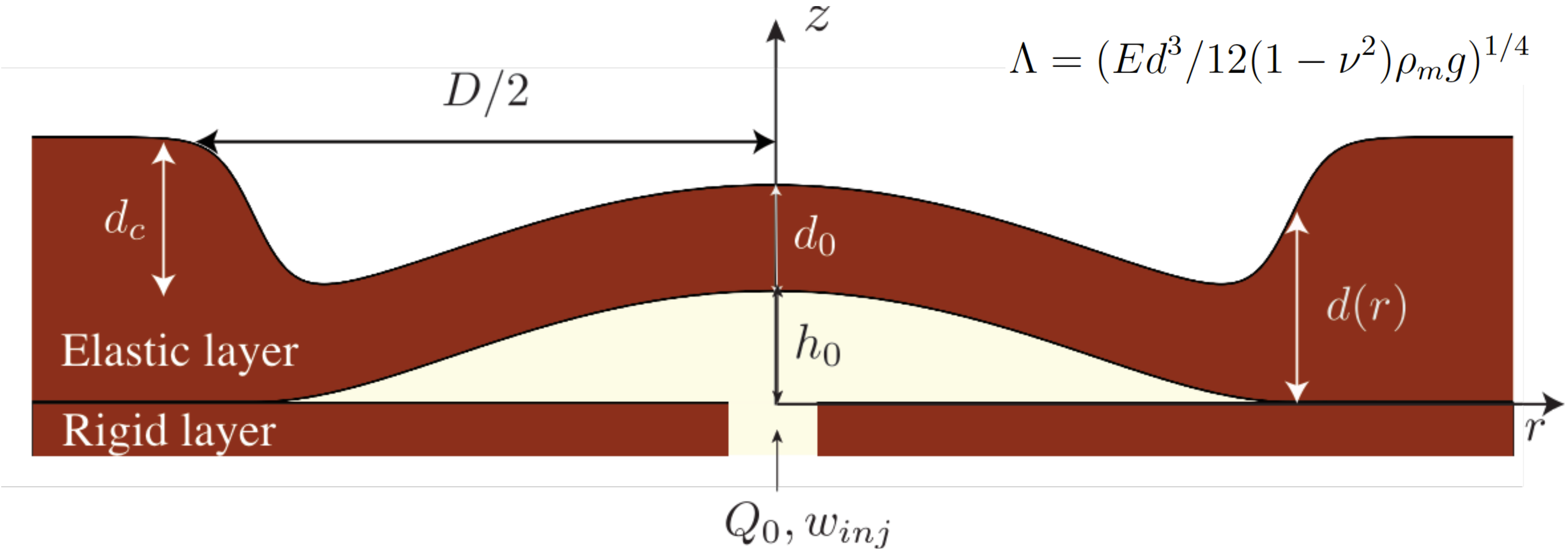

$$\frac{\partial h}{\partial t} = \frac{\rho_m g}{12\mu}\frac{1}{r}\frac{\partial}{\partial r}\left(rh^3\frac{\partial h}{\partial r}\right) + \frac{\rho_c g}{12\mu}\frac{1}{r}\frac{\partial}{\partial r}\left(rh^3\frac{\partial d(r)}{\partial r}\right)$$
$$+\frac{E}{144\mu(1-\nu^2)}\frac{1}{r}\frac{\partial}{\partial r}\left(rh^3\frac{\partial}{\partial r}\nabla_r^2 d(r)^3\nabla_r^2 h(r)\right) + w(r,t)$$

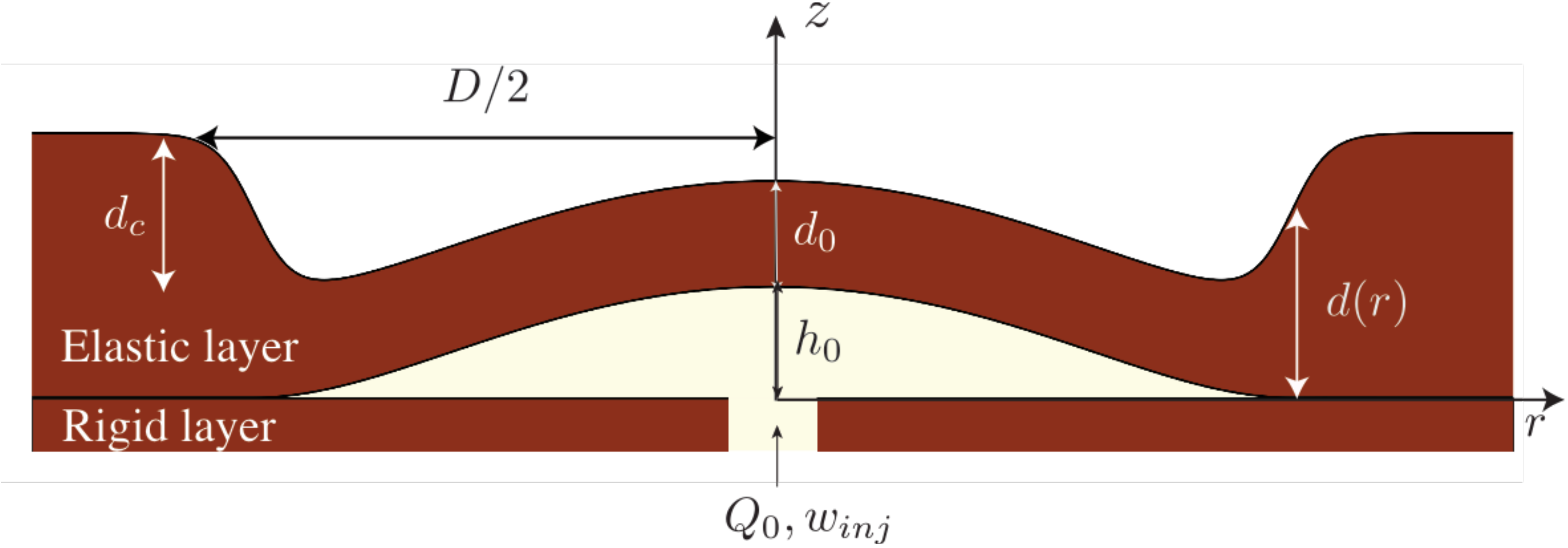

Intrusion shape and floor appearance depends on

$$\frac{4\Lambda}{D/2}$$

$$\frac{4\Lambda}{D/2} > 1$$

$$\frac{4\Lambda}{D/2} < 1$$

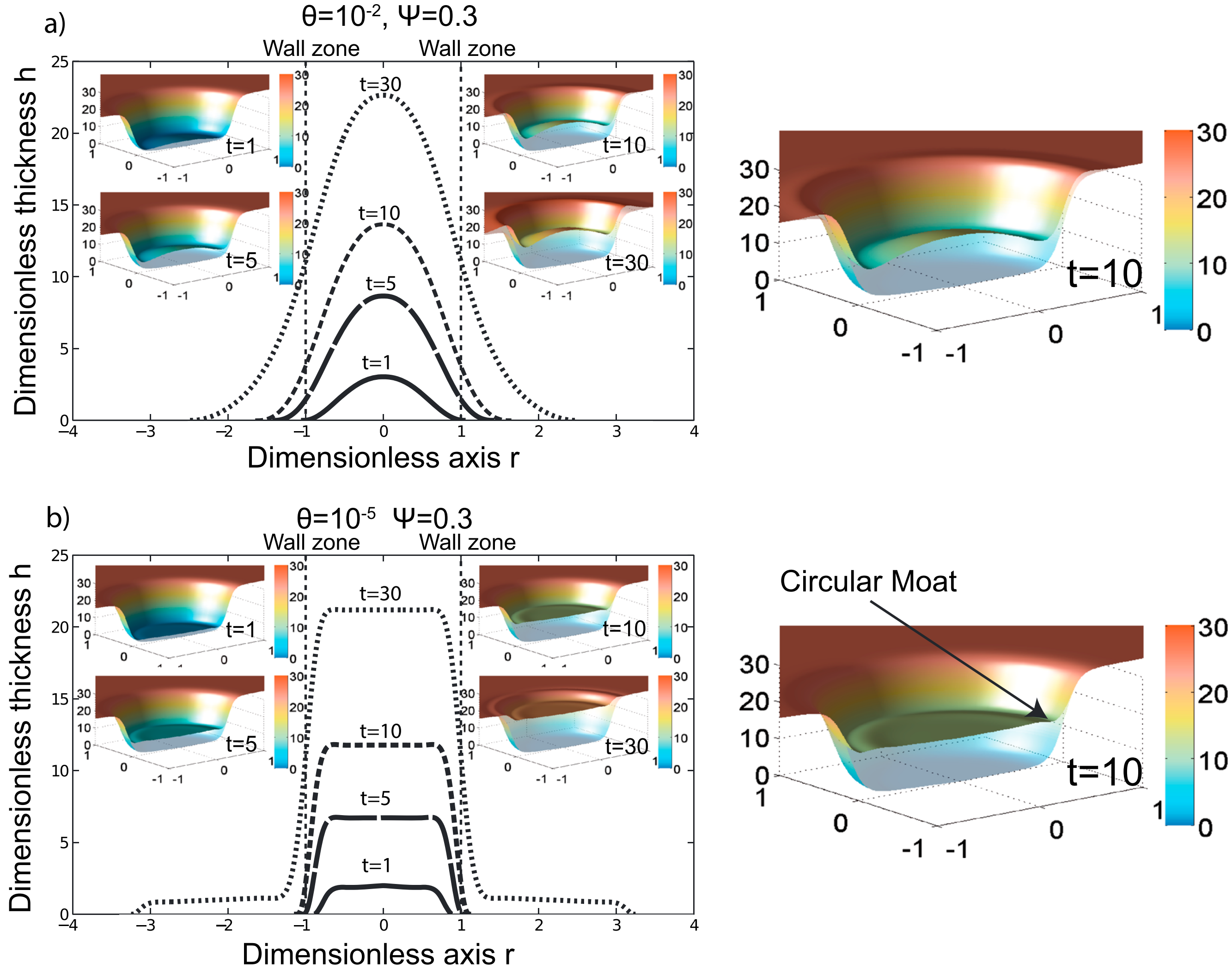

Thorey & Michaut, JGR 2014

$$\frac{4\Lambda}{D/2} > 1$$

$$\frac{4\Lambda}{D/2} < 1$$

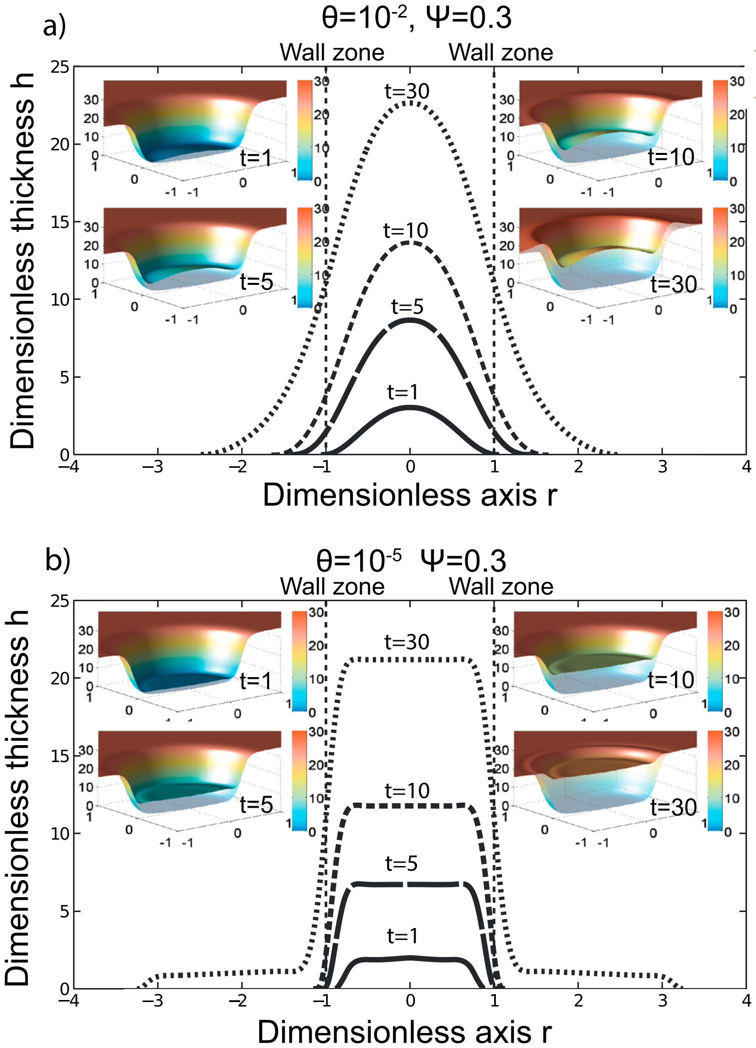

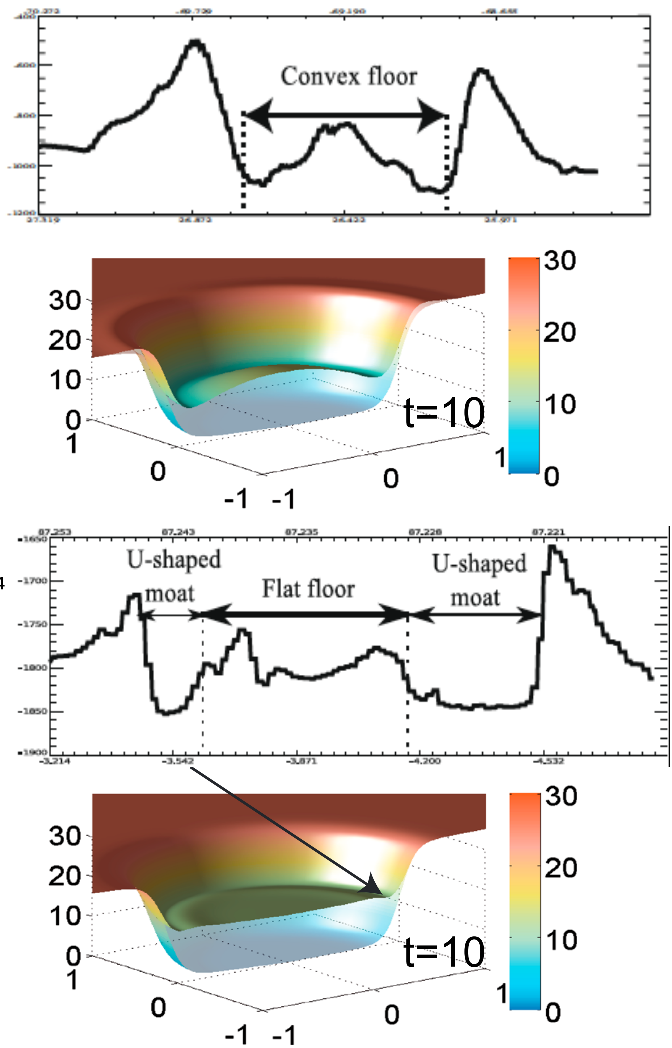

Thorey & Michaut, JGR 2014

$$\frac{4\Lambda}{D/2} > 1$$

$$\frac{4\Lambda}{D/2} < 1$$

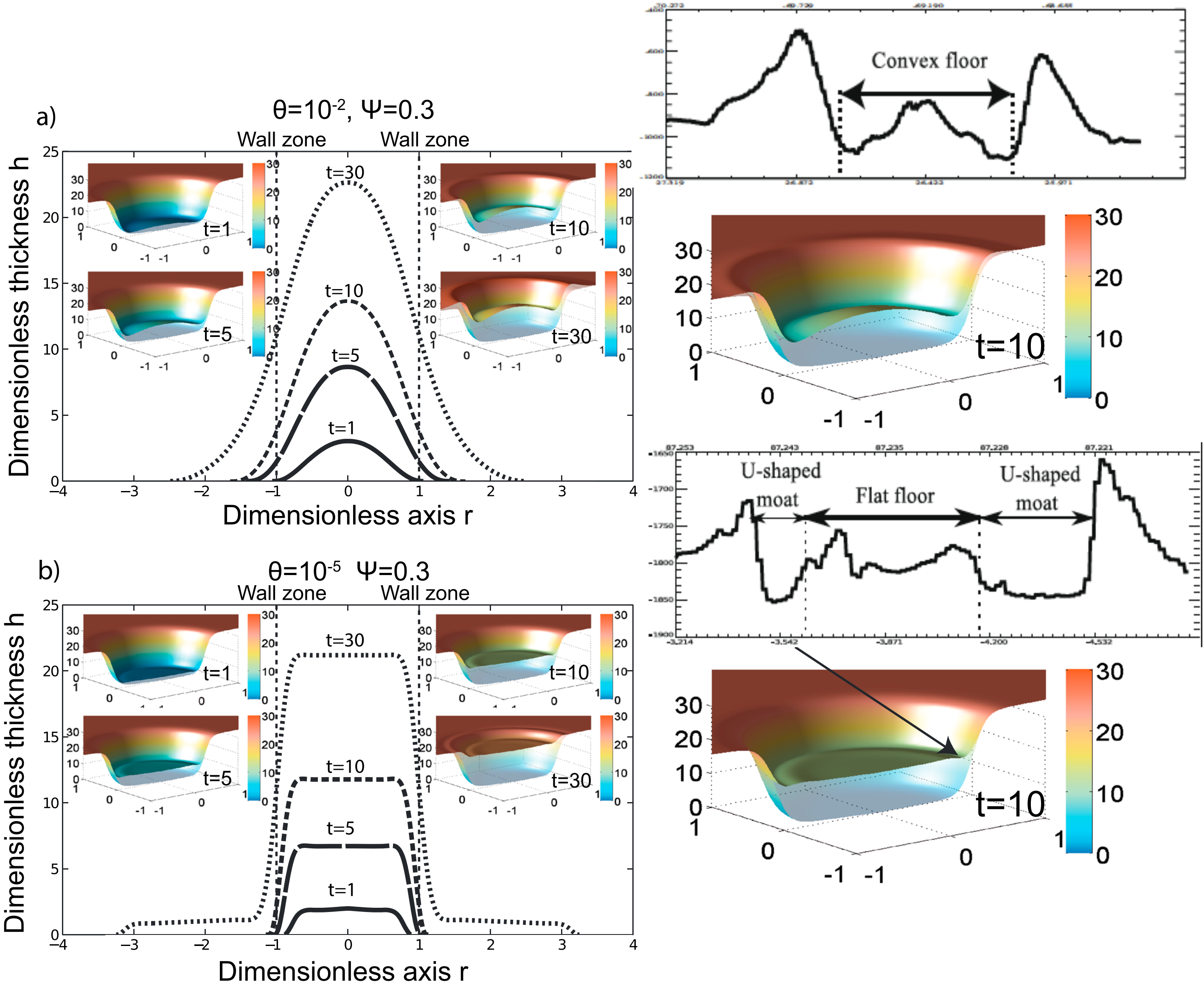

Shallow magmatic intrusions are present below floor-fractured craters

Thorey & Michaut, JGR 2014

Examples of applications: low-slope lunar domes

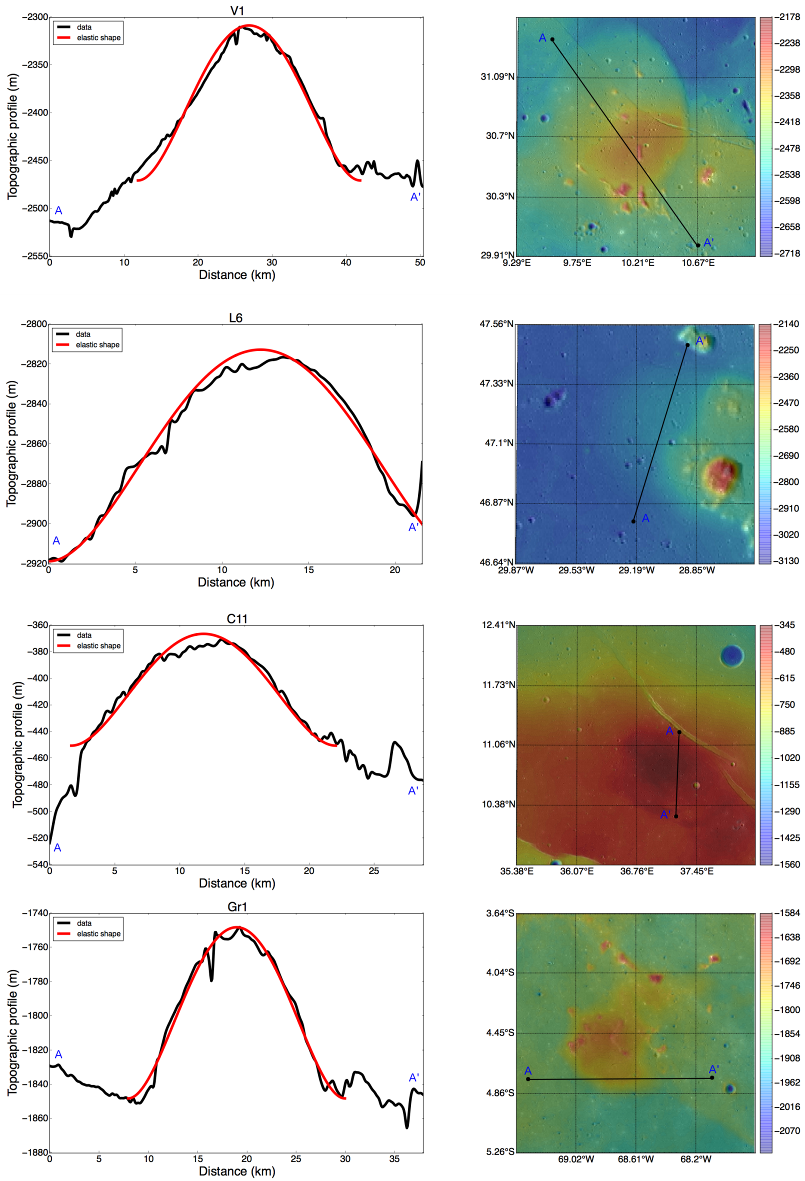

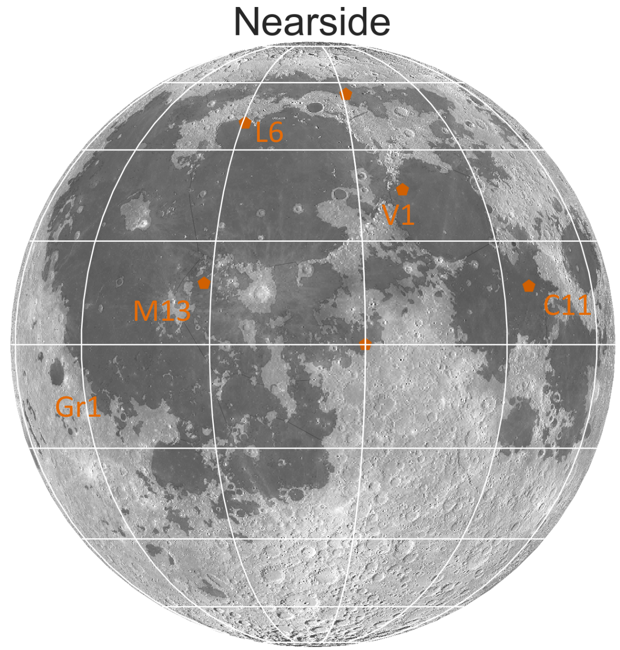

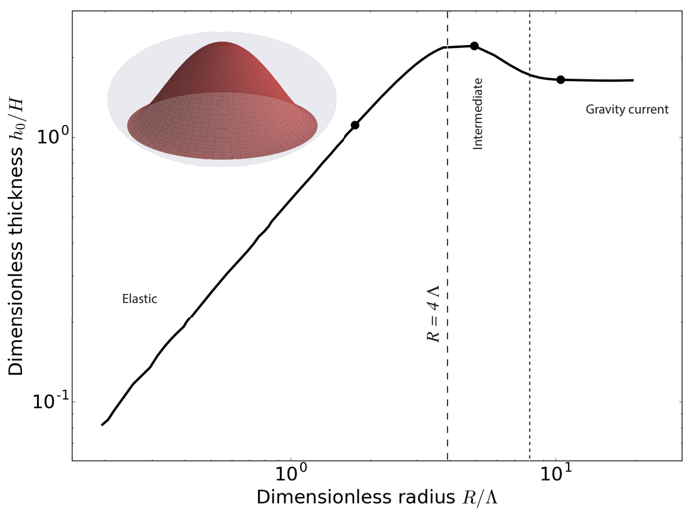

Data: Wöhler et al (2009)

Examples of applications: low-slope lunar domes

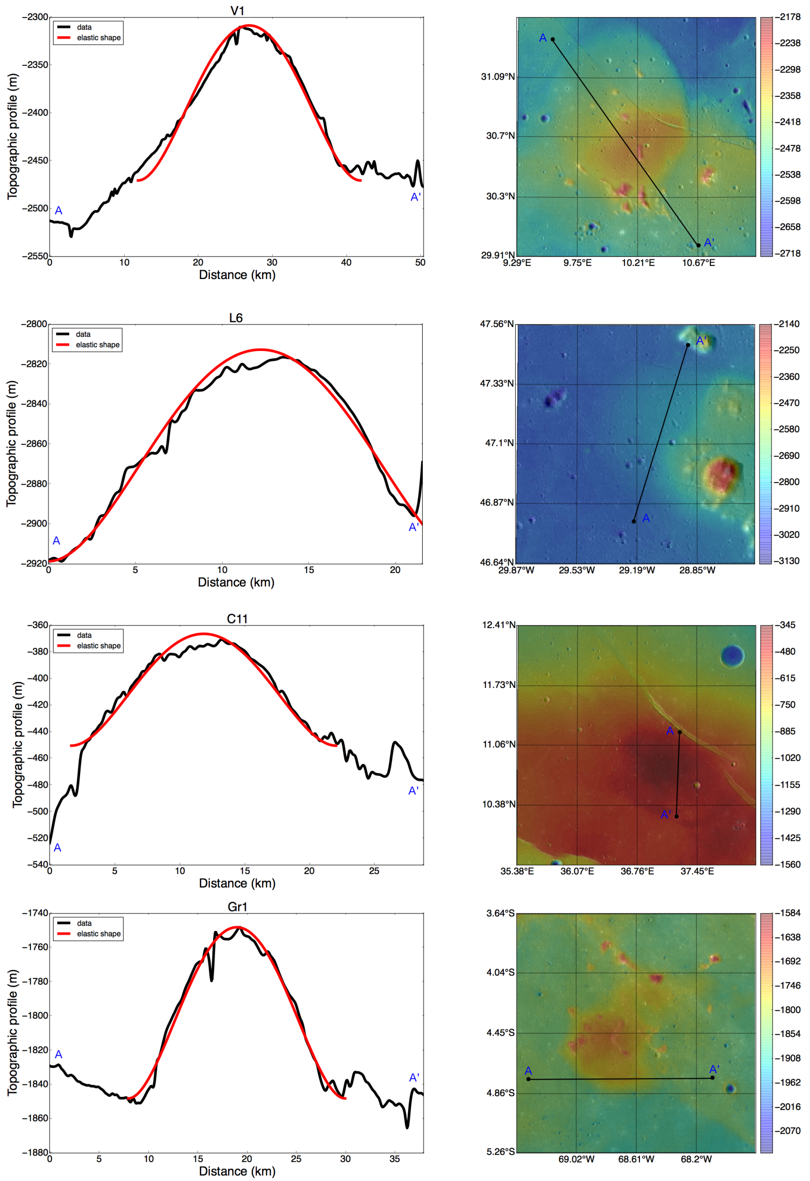

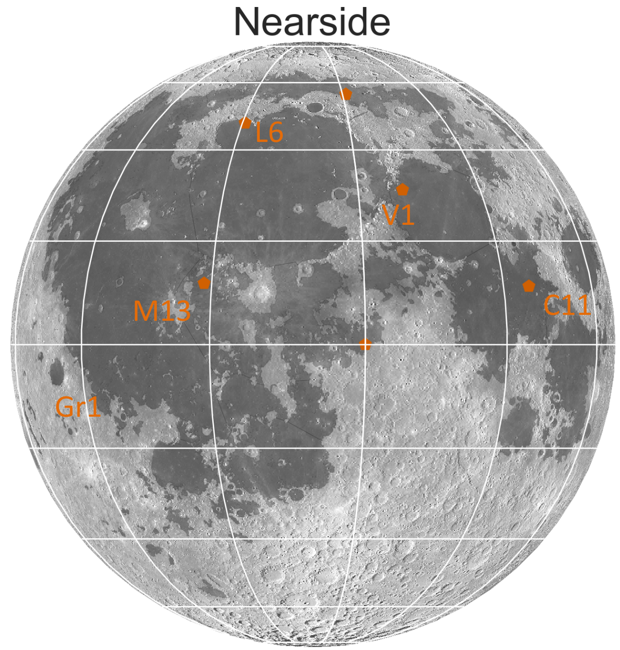

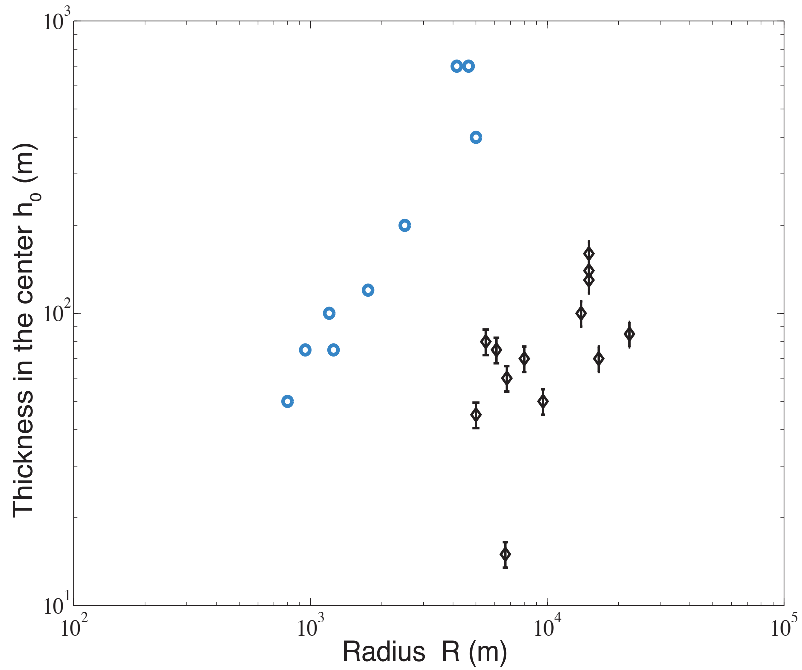

Data: Rocchi et al (2002), Wöhler et al (2009)

Examples of applications: low-slope lunar domes

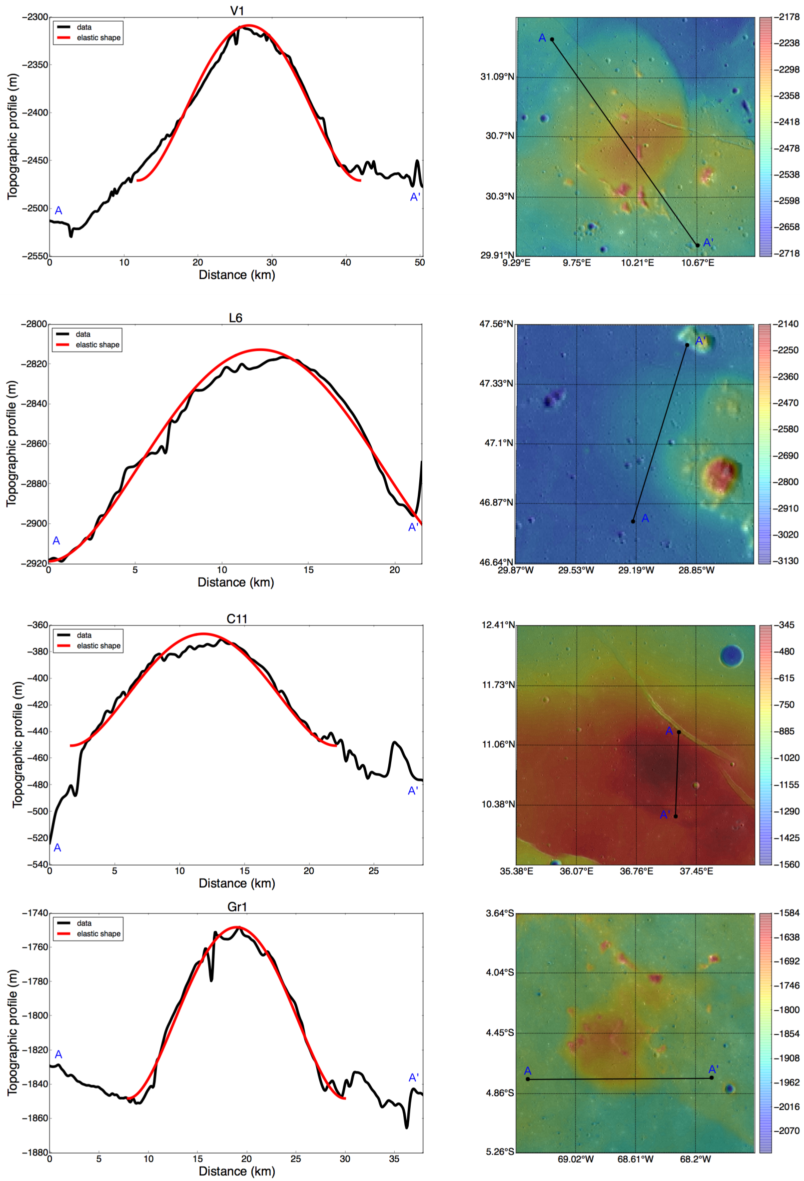

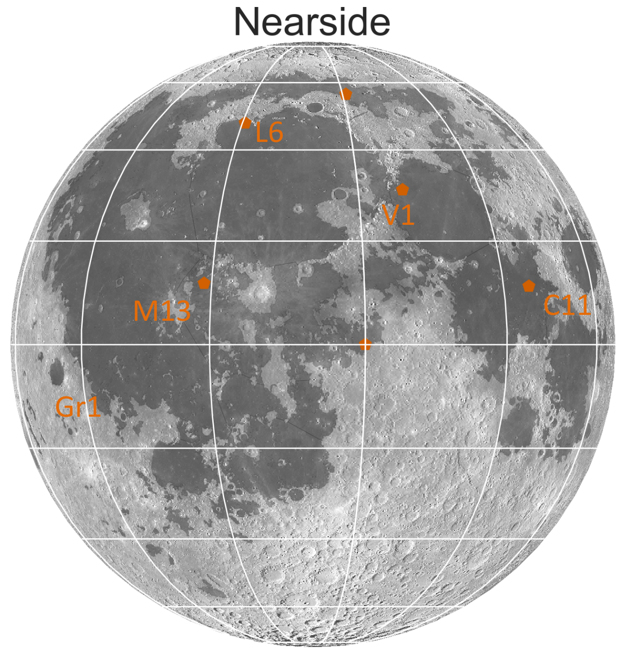

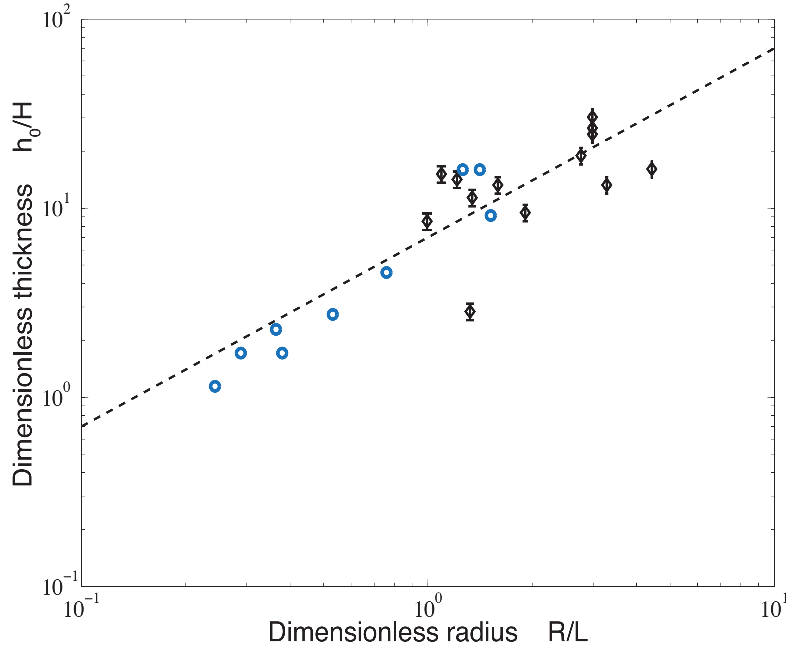

Data: Rocchi et al (2002), Wöhler et al (2009)

Constraints on mare basalt thicknesses

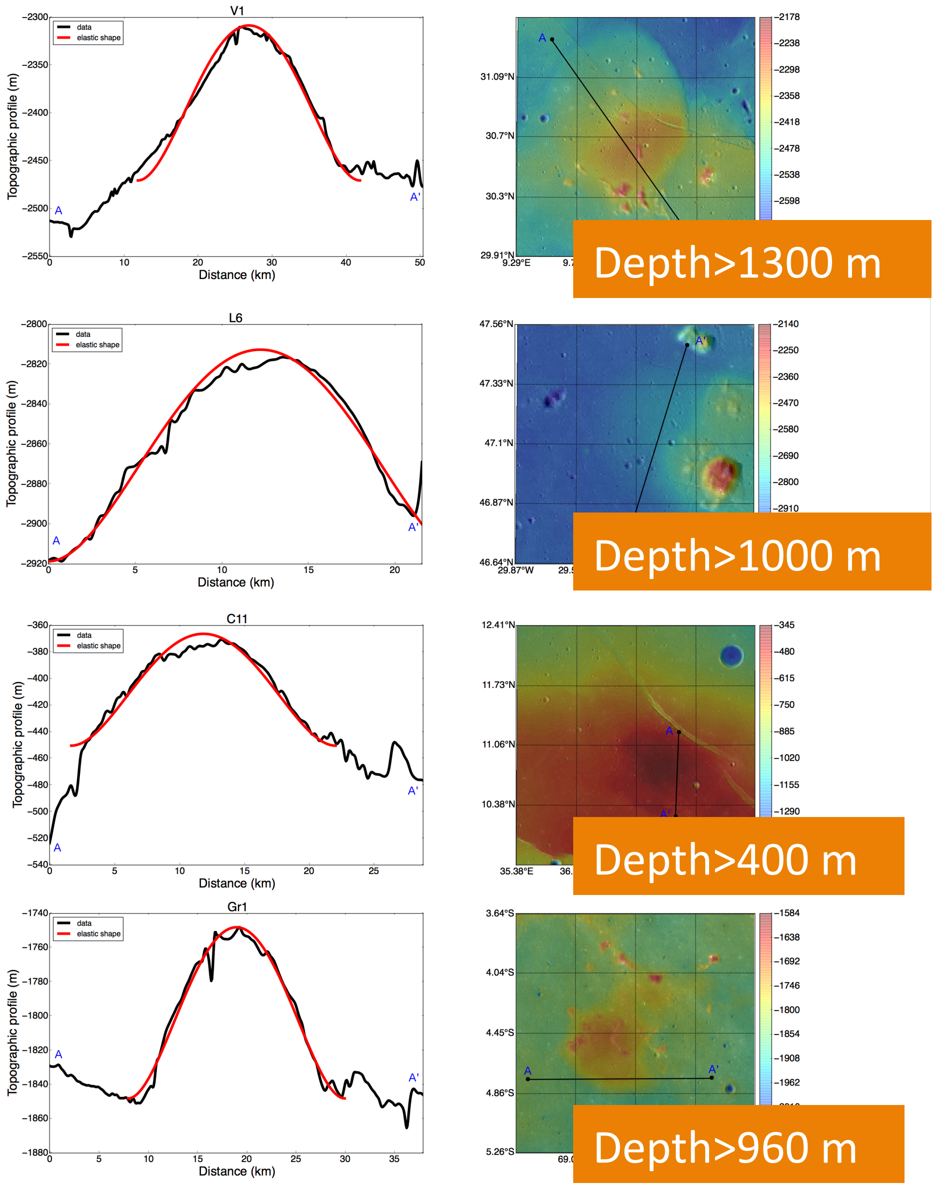

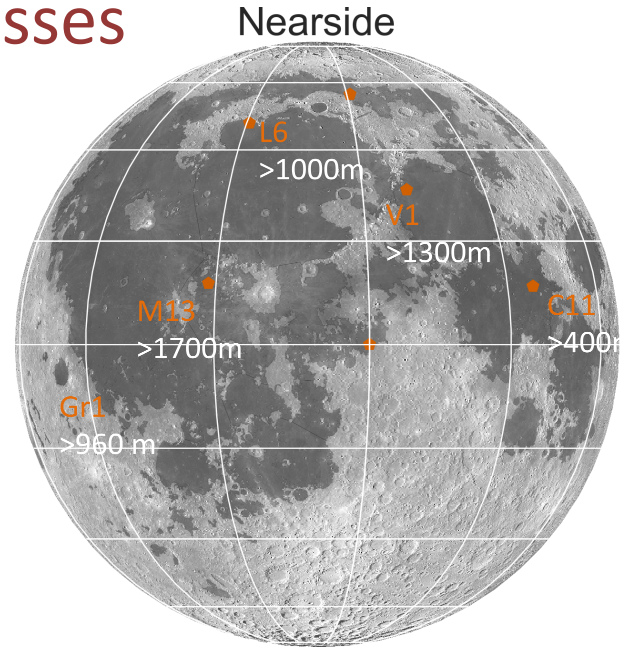

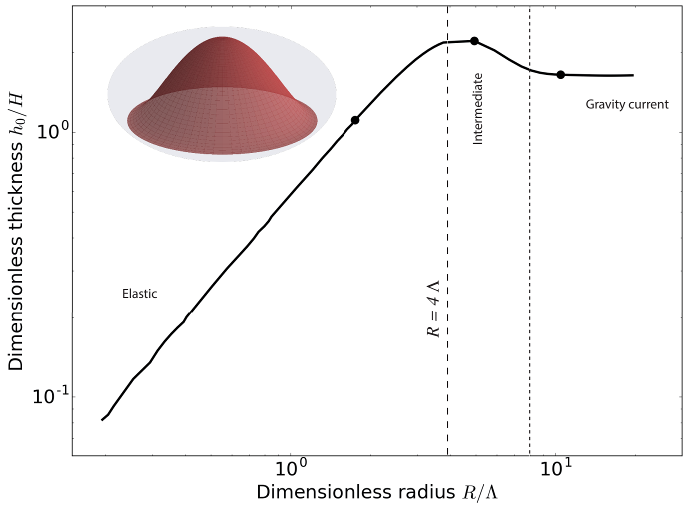

$$R < 4\Lambda \Rightarrow d > \left(\frac{3(1-\nu^2)\rho g R^4}{4^3 E} \right)^{1/3}$$

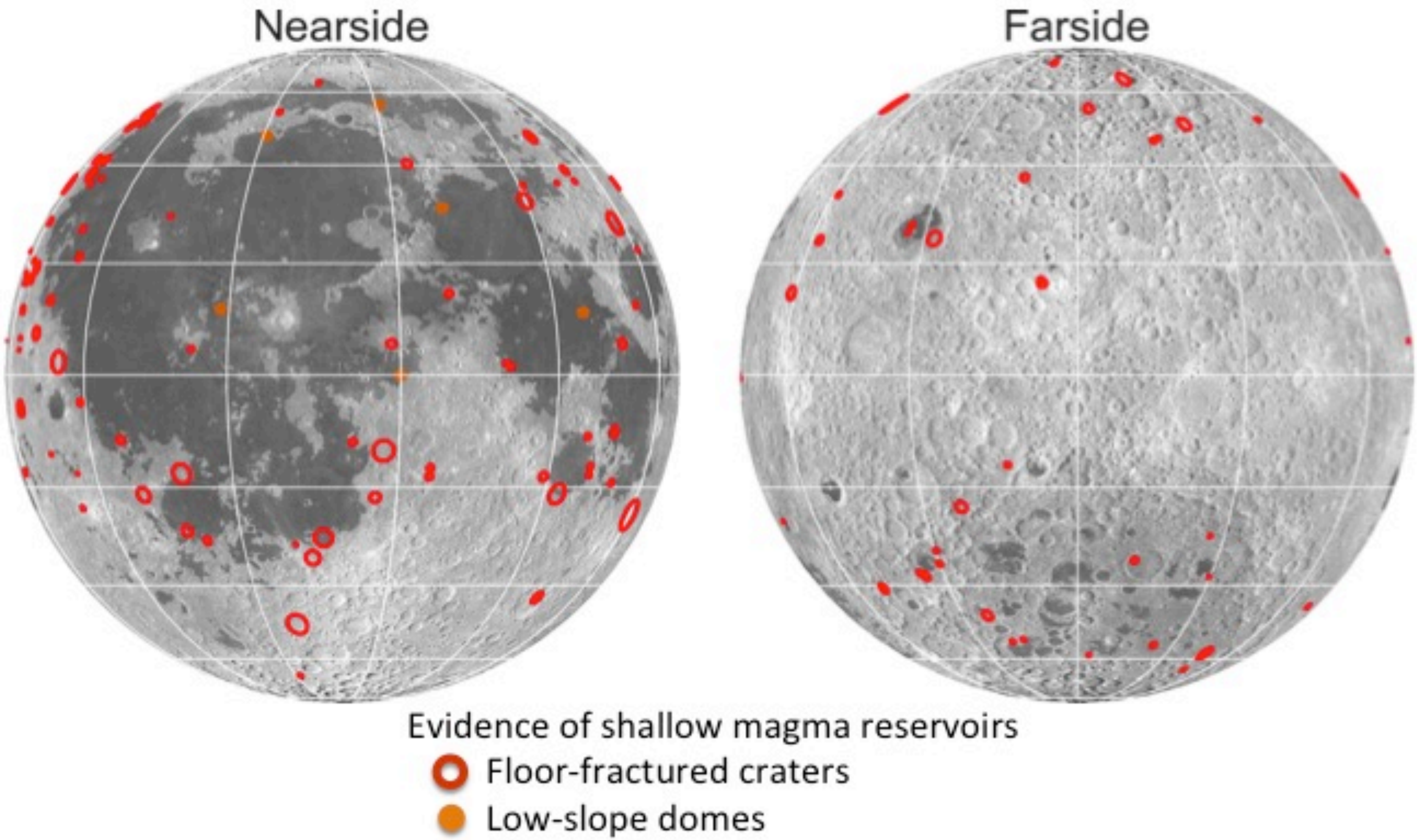

A lot of evidence of shallow solidified magma reservoirs at the surface of the Moon, mostly below craters and surrounding mare basalt area.

Conclusions

- Laccoliths spreading is controlled by the elastic deformation of the overlying plate.
- Laccoliths' shapes provide information on their depth.
- Cooling significantly slows down their spreading by rapidly increasing the viscosity of the tip.
- Topography also influences the spreading of shallow intrusions.
- Shallow intrusions are numerous in the lunar crust.

Cooling

Temperature-dependent viscosity

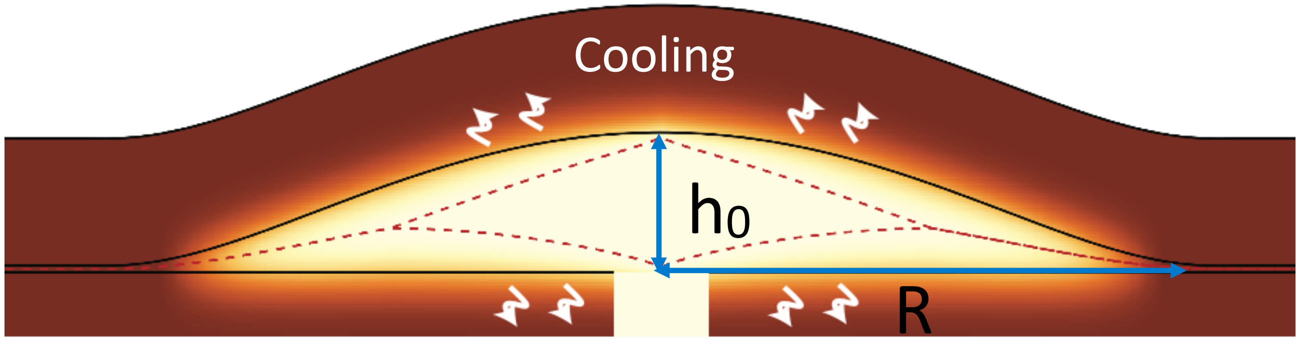

$$\nu = \frac{\eta_{\rm hot}}{\eta_{\rm cold}}$$

$$Pe = \frac{HQ_0}{\pi\kappa\Lambda^2}$$

$$\eta(T) = \frac{\eta_h \eta_c (T_i - T_0)}{\eta_h (T_i - T_0) + (\eta_c - \eta_h)(T - T_0)}$$

Potential gravitational signature of FFCs

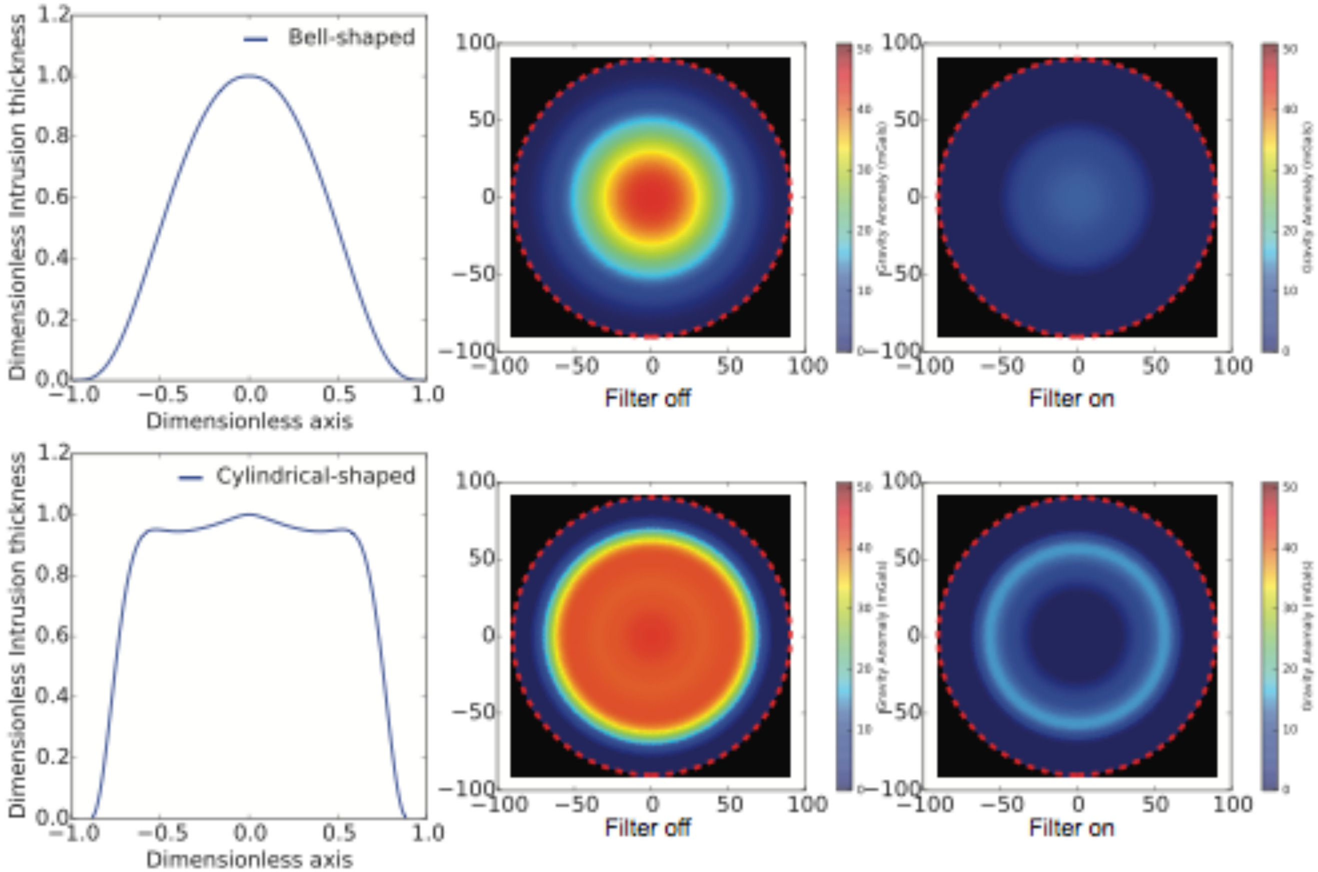

h_0 = 2 km
$\Delta\rho$ = 500 kg m^{-3}

Thorey, Michaut and Wieczorek, EPSL 2015

Gravitational signature of FFCs: GRAIL's data

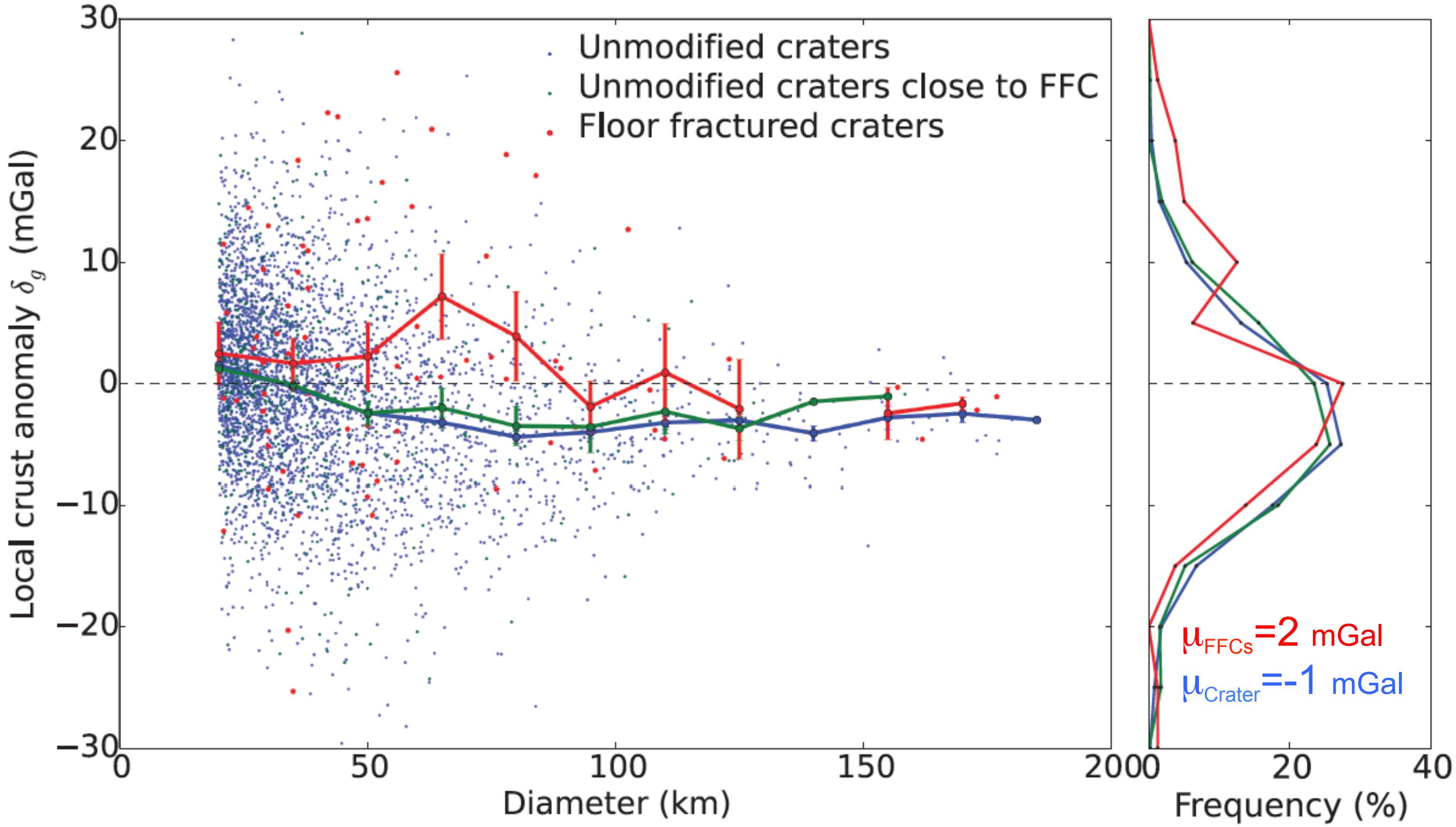

Thorey, Michaut and Wieczorek, EPSL 2015

Gravitational signature of FFCs: GRAIL's data

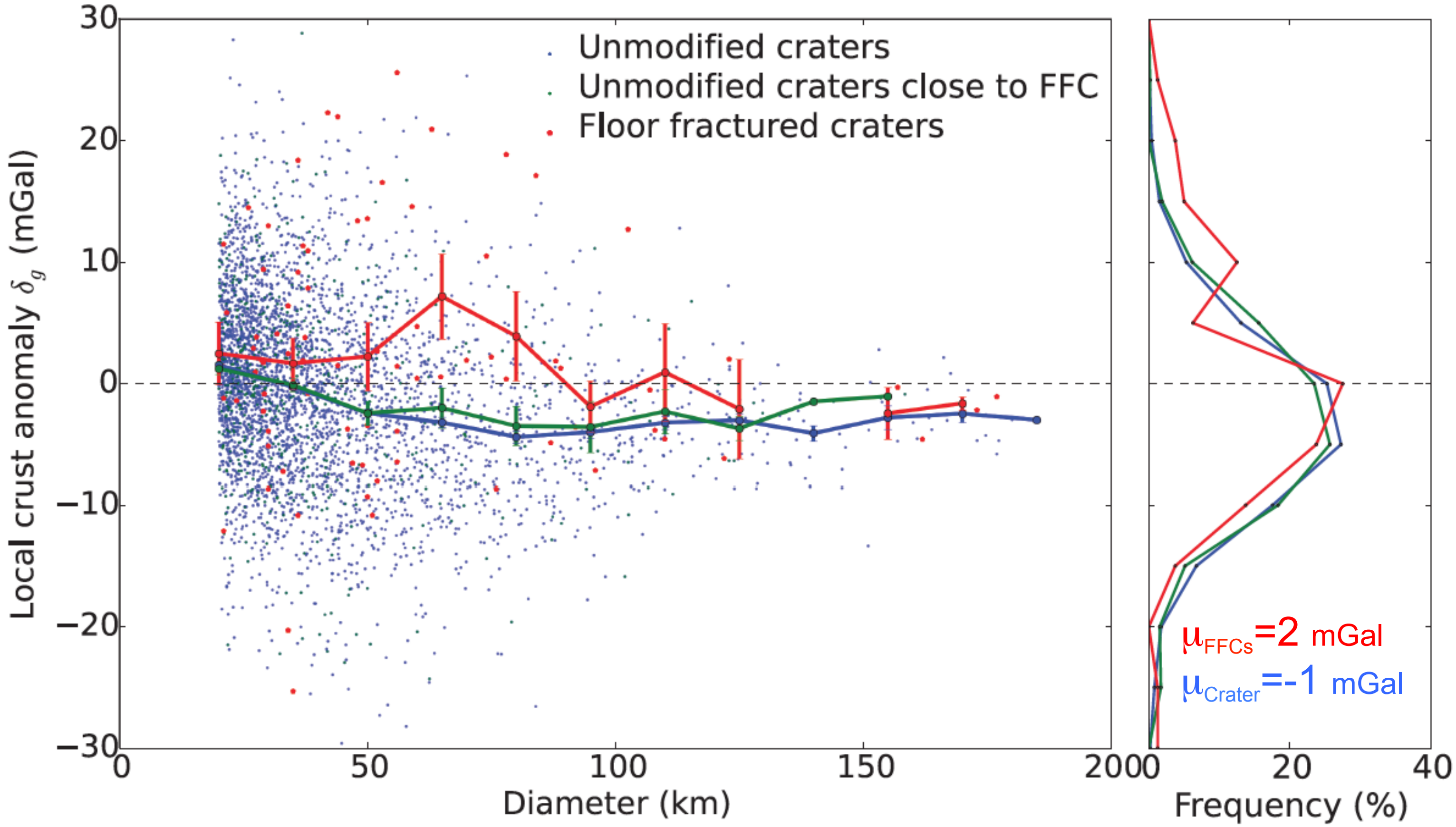

GRAIL's data confirm the presence of intrusions below floor-fractured craters

Thorey, Michaut and Wieczorek, EPSL 2015